Combustion and Flame 228 (2021) 13–28

Contents lists available at ScienceDirect

Combustion and Flame

journal homepage: www.elsevier.com/locate/combustflame

An experimental and kinetic modeling study on the laminar burning velocity of NH_3+N_2O+air flames

Xinlu Han[a,b], Marco Lubrano Lavadera[a], Alexander A. Konnov[a,*]

[a] Division of Combustion Physics, Lund University, Lund SE 22100, Sweden
[b] State Key Laboratory of Clean Energy Utilization, Zhejiang University, Hangzhou 310027, PR China

ARTICLE INFO

Article history:
Received 27 November 2020
Revised 13 January 2021
Accepted 13 January 2021
Available online 30 January 2021

Keywords:
Laminar burning velocity
Ammonia
Nitrous oxide
Kinetic mechanism

ABSTRACT

In the present work, the laminar burning velocities of the NH_3+N_2O+air flames were measured using the heat flux method at 1 atm and 298 K, with varied equivalence ratios and N_2O mixing ratios. For the mixing ratio $N_2O/(N_2O+air)$ = 0.5, a full range of equivalence ratios was covered. Moreover, at three equivalence ratios an extended range of mixing ratios was investigated. The laminar burning velocity has an approximately linear relationship against the fraction of nitrous oxide in the oxidizer mixture, regardless of the tested equivalence ratios. Several recently published NH3 mechanisms were compared with these new experimental data; among them the models of Nakamura et al. and Stagni et al. show the best performance for NH_3+N_2O+air flames over the entire range of the mixing ratios. The H/N/O kinetic mechanism of the authors was analyzed and updated focusing on the rate constants of reactions most sensitive in ammonia flame propagation and self-ignition of NH_3+O_2 and H_2+N_2O mixtures. The choice of the new rate constants is outlined, however, no modification (adjustment or tuning) of the rate parameters to accommodate experimental results was attempted. The updated mechanism demonstrates significantly improved agreement with all measurements used for the model development and with other experimental data from the literature for ammonia flames and self-ignition. A comparative reaction path analysis for NH_3+N_2O+air and NH_3+air flames revealed that an almost linear increase of the laminar burning velocity with an increased fraction of N_2O in the oxidizer originates from the rate controlling reaction N_2O+H = N_2+OH, which produces OH radicals dominating ammonia oxidation.

1. Introduction

Recently revitalized interest in ammonia (NH_3) as a potential renewable and carbon-free fuel has motivated numerous test studies in engines [1] and gas turbines [2], as well as laboratory research on fundamental combustion properties such as ignition delays and flame propagation in pure ammonia and blended fuel mixtures. The major obstacle for the direct utilization of NH_3 in combustion systems is largely different characteristics compared to common hydrocarbon fuels: the higher heat of vaporization, the lower heating value, higher minimum ignition energy, higher auto-ignition temperature, much slower burning velocity, narrow flammability range, lower adiabatic flame temperature, higher ignition delay time, low radiation intensity, and slow chemical conversion rate [3]. Therefore, a detailed understanding of the high-temperature chemistry of ammonia is required both to predict the behavior of NH_3 in industrial combustors and to propose new approaches overcoming these limitations or modifying combustion regimes.

Nowadays, various kinetic mechanisms are available in the literature to describe the combustion and ignition properties of NH_3, all of them based on the fundamental review of Miller and Bowman [4], however, uncertainties are retained in the key reactions governing ammonia oxidation, and predictions using different mechanisms could have significant deviations among each other. Figure 1 shows examples of the laminar burning velocity (S_L) calculations of NH_3+air flames at 1 atm and 298 K using several contemporary models. The tested kinetic mechanisms are from Glarborg et al. [5], Okafor et al. [6], Shrestha et al. [7], Nakamura et al. [8], Otomo et al. [9], Mei et al. [10], Mathieu and Petersen [11], Han et al. [12], Li et al. [13], Stagni et al. [14], and recently updated model of the authors [15,16], which in the following, is called Model 1 to avoid confusion with other models developed in Lund. Experimental data from the literature are shown for comparison, which are taken from Takizawa et al. [17], Ronney

* Corresponding author.
E-mail address: alexander.konnov@forbrf.lth.se (A.A. Konnov).

https://doi.org/10.1016/j.combustflame.2021.01.027

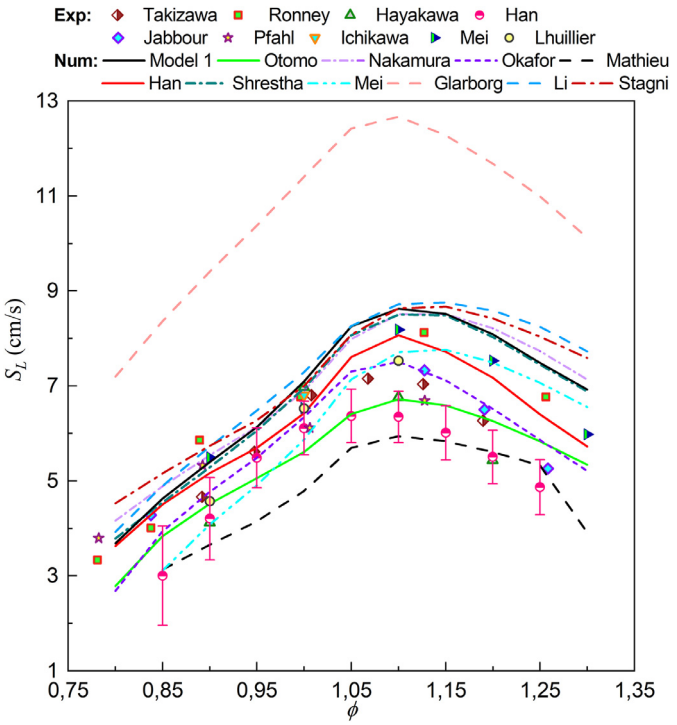

Fig. 1. Laminar burning velocities of NH_3+air flames at 1 atm and 298 K. Symbols: experiments, lines: numerical modeling.

[18], Pfahl et al. [19], Jabbour et al. [20], Han et al. [21], Hayakawa et al. [22], Ichikawa et al. [23], Mei et al. [10], and Lhuillier et al. [24]. As seen in Fig. 1, at equivalence ratio, ϕ, close to 1.1 the variation of the predicted burning velocities is from ~5 to ~12 cm/s, while the experimental S_L values scatter from 6 to 8 cm/s. An experimental uncertainty, which at the best is close to ± 1 cm/s [21] is, therefore, relatively high that, together with the spread of the burning velocities themselves hampers validation of detailed kinetic models. It should be noted that radiation heat losses were taken into account in the modeling presented in Fig. 1, because they influence the calculated burning velocities of the slowly burning flames as will be detailed in the following.

Since the experimental uncertainty does not change much when the laminar burning velocity grows [25], it would be more convenient to target conditions with larger S_L. The simplest way to achieve higher burning velocities of ammonia, which is also considered as a practical approach to implement it in industrial combustors, is to mix it with methane (natural gas) [21,6,26,27] or with syngas[28,12,29]. The use of these experimental data for model validation, however, requires complete H/C/N/O mechanisms where quality and performance of the hydrocarbon kinetics is crucial for the analysis of the possible deficiencies in the H/N/O submodel itself. More convenient is to investigate binary fuel mixtures of NH_3+H_2 [21,24,29], or to increase the unburnt mixture temperature [24,30,31]. Also possible is to substitute part or all of N_2 in air by O_2 [10,30,32], or to use NO as an oxidizer instead of air [33–35]. In all these cases the differences between calculated burning velocities enlarge with larger S_L that facilitates model validation and analysis.

Another option to increase the laminar burning velocities of ammonia, explored in the present study, is to use nitrous oxide, N_2O, as an oxidizer. Shock tube studies in the system NH_3+N_2O have a long history and originally focused on self-ignition phenomena [36–39]. Deflagration to detonation transition in NH_3+N_2O mixtures was also studied [40] and an increase from 0–0.6 m/s at the initial ignition stage up to detonation velocity of 2198 m/s was reported. In the kinetic experiments with diluted mixtures [41,42], nitrous oxide was a source of O atoms that allowed to derive rate constants of reactions between ammonia and O atoms or OH radicals. Flame structure of the low-pressure (0.079 atm) NH_3+N_2O+Ar flame using laser-induced fluorescence and mass spectrometry was reported by Venizelos and Sausa [43]. They suggested several modifications to the Miller and Bowman mechanism [4] and demonstrated good agreement between the modeling and their experiments.

The first measurements of the burning velocity of NH_3+N_2O mixtures were performed by Van Tiggelen and colleagues [44–46], who used the flame cone method and different dilutions by N_2 to change the flame temperature and obtain effective activation energy of the flame propagation. They found a linear correlation between the diluent content and S_L, and noted that the maximum burning velocity is observed in slightly lean mixtures. Parker and Wolfhard [34] reported burning velocities in the range from 0.04 to 1 atm where S_L slightly increases with pressure and compared this trend with other flames supported by NO and NO_2. Gray and colleagues [47–49] investigated low-pressure (0.091 atm) spherical flames of NH_3+N_2O mixtures as well as ternary mixtures with O_2 and H_2 at an initial gas temperature of 333 K. The burning velocity was derived from the flame radius vs. time records recalculated using density ratio of the products and reactants. The authors [47,48] concluded that their results agree with the earlier studies [44,45,34] both in the absolute values of S_L and the position of the maximum, though significant experimental uncertainties (± 30%) were considered possible. The measurements of Andrews and Gray [47] were further revisited by Brown and Smith [50], who essentially performed stretch correction comparing calculated flame speeds in spherical and planar 1D flames implementing the kinetic model of Miller and Bowman [4]. They found that for NH_3+N_2O mixtures minor correction is needed in lean flames, while in stoichiometric and rich flames it exceeds 10%, and evaluated the uncertainty of the modified S_L be around 15%. Investigation of Pfahl et al. [19] was focused on flammability limits, and ignition energy of H_2–CH_4–NH_3–N_2O–O_2–N_2 mixtures at standard conditions motivated by safety concerns. They also obtained burning velocities of NH_3+air flames shown in Fig. 1 as well as of NH_3+N_2O+air flames with nitrous oxide content up to 8% and noted a significant increase of S_L caused by N_2O addition. Pfahl et al. [19] observed the dramatic effect of buoyancy on the development and shape of slowly burning initially spherical flames and suggested that the difference of the burning velocity within ± 1 cm/s with the measurements of Ronney [18] performed in microgravity is reasonable.

One may expect, therefore, that investigation of NH_3+N_2O+air flames could considerably reduce the relative uncertainty of the burning velocity measurements allowing for better screening and validation of kinetic models, moreover, the presence of nitrous oxide should modify the importance of the key reactions controlling flame propagation. Figure 2 shows the most sensitive reactions from the recently updated model of the authors [15,16] (Model 1) for the laminar burning velocities of stoichiometric NH_3+air, NH_3+H_2+air, NH_3+O_2+N_2, NH_3+NO, and NH_3+N_2O+air flames at 1 atm and 298 K. Although different mixtures share almost the same sensitivity spectra, some reactions appear most critical at specific conditions which can help improving model behavior via analysis and updates of their rate constants following the approach of Brown and Smith [50]. On the other hand, this also indicates the need for concerted validation of the kinetic mechanism performance using different experiments to avoid modifications that can bring it in agreement with one dataset but deteriorate modeling capabilities at other conditions. To this end, in the present work, the laminar burning velocities of NH_3+N_2O+air mixtures of different composition were obtained using the heat flux method at 1 atm and initial gas temperature of 298 K. Several detailed

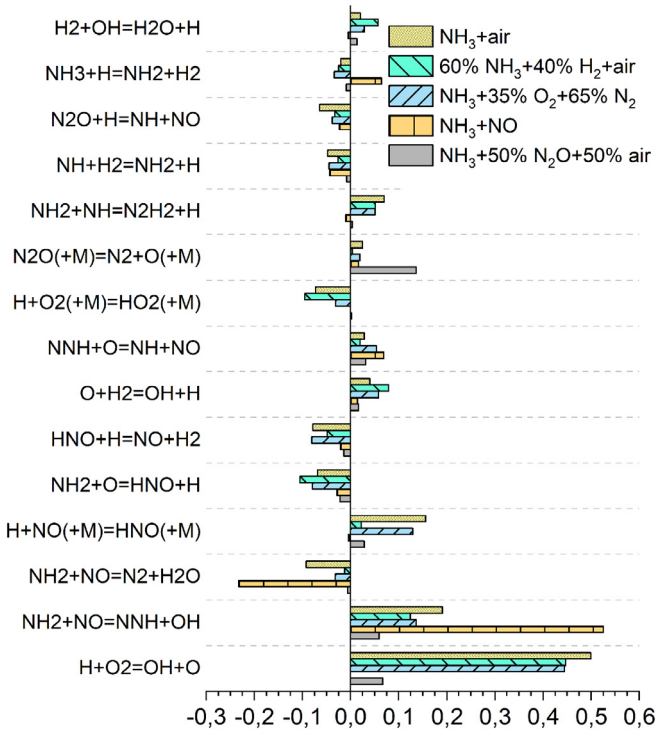

Fig. 2. Normalized A-factor reaction sensitivities of the laminar burning velocities for stoichiometric NH_3+air, NH_3+H_2+air, NH_3+O_2+N_2, NH_3+NO, and NH_3+N_2O+air flames at 1 atm and 298 K (compositions in mole basis).

kinetic schemes were tested and the model of the authors was updated considering S_L measured in other ammonia flames mentioned above, as well as selected ignition delay data from the literature. Due to the availability of a large number of detailed models for ammonia combustion, they were first screened by analysis of their previous validation for combustion of mixtures containing NH_3 and/or N_2O relevant to the present study. Further examination of the most sensitive reactions is used to improve the prediction abilities of the model of the authors. However, the goal to achieve a perfect match with the measurements was not pursued. Finally, the reaction pathway analysis is used to prove that the burning velocities of NH_3+N_2O+air flames provide an important independent target for the validation and development of detailed kinetic models.

2. Experimental details

The heat flux method for measuring burning velocities implemented in the present study has many advantages and some limitations fully documented by Alekseev et al. [51]. Specific shortcomings related to the stabilization of ammonia flames have been discussed in our recent works [12,21,52]. First, NH_3 can be corrosive towards brass which typical heat flux burners are made from. Therefore, the burner of the old design designated “E2” [51] has been used. With this burner, the temperature of the heating jacket is controlled by a hot water circuit that hampers stabilization of the flames having very low (below 10 cm/s) burning velocities. Thus the measurements of the burning velocities of NH_3+air flames (performed by Han et al. [12,21] using the heating circuit with oil) or flames with a small amount of N_2O added to the mixture were not possible. Second, the upper limit of S_L is dictated by the perforation pattern of the burner plate, which for 0.5 mm-diameter holes at a pitch of 0.7 mm is about 50–60 cm/s [51]. This prevents from covering a complete range of stoichiometric compositions for NH_3+N_2O flames, for which at $\phi = 1$ the burning velocity is close to 80 cm/s [34].

Table 1
Experimental conditions covered in the present study for NH_3+ N_2O+air mixtures.

Mixing ratio x_{N2O}	Equivalence ratio ϕ
0.5	0.4–2.0
0.3–1.0	0.6
0.15–0.65	1.0
0.2–0.8	1.4

Thus, in the present study NH_3+N_2O+air flames with varied equivalence ratios and N_2O mixing ratios were investigated. The N_2O was considered as part of the oxidizer and its content was denoted as $x_{N2O} = N_2O/(N_2O+air)$. The equivalence ratio was calculated such that complete combustion products are N_2 and H_2O. Table 1 shows all experimental conditions visited, where the increment of x_{N2O} in each dataset is 0.05 while that of ϕ is 0.1.

The descriptions of the heat flux burner, experimental setup and experimental procedures can be found in the previous publications [53,15]. The uncertainty of the measured S_L was evaluated from the radial temperature scattering in the burner plate measured by eight thermocouples and the uncertainties of the mass flow controllers as described by Alekseev et al. [51]. An additional uncertainty has been introduced due to the uncertainty in the effective perforation area of burner “E2” discussed in details in our recent work [52], which leads to a higher uncertainty of measured S_L than commonly reported for measurements performed with the heat flux method (usually $<$ 1 cm/s). All experimental data with associated uncertainties are tabulated in the Supplemental Material.

3. Modeling details

Premixed flame modeling as well as sensitivity and reaction pathway analyses were performed using ANSYS Chemkin 17.0 software [54]. The laminar burning velocity was calculated considering multicomponent transport and thermal diffusion options. A grid-independent solution was ensured by setting the parameters GRAD and CURV to 0.02 and 0.05, respectively, resulting in a number of grid points around 500–700 over the domain of 3 cm. Radiation heat losses were taken into account because they influence the calculated burning velocities of the slowly burning flames as demonstrated by Nakamura and Shindo [55]. The modeling of the radiation heat losses in ANSYS Chemkin assumes that the radiation is from an optically thin layer, and the radiation from NO, NH_3, N_2O, and H_2O was considered in the present study. It should be noted that among the five tested mechanisms described below, only the present mechanism and that of Nakamura et al. [8] include the absorption coefficients of the radiative species. On the other hand, the radiation heat losses have a very small impact (less than 0.2 cm/s) on the calculated burning velocities of NH_3+N_2O+air mixtures studied in the present work, and could be noticeable only in very lean and very rich NH_3+air mixtures [55]. The experimental ignition delay times by Mathieu and Petersen [11] and Mulvihill et al. [56] were defined using a slope of OH* emission profile; the same procedure was used in the modeling.

The modeling has been initially performed using the recently updated model of the authors [15,16] (Model 1), which will be described and eventually improved in the following. Besides, four kinetic mechanisms from the literature were tested. This selection is based on the recent comparative study of detailed reaction mechanisms for ammonia combustion [57] and an additional analysis summarized in Table 2. It should be noted that even the lists of considered kinetic models covered by Kawka et al. [57] and in the present work are not the same since several mechanisms were

Table 2
Most recent kinetic models and experiments relevant to the present work.

Mechanism	Year	Comparison with experiments					
		Laminar burning velocity				ST ignition delay time	
		NH_3+air	NH_3+H_2+air	NH_3+O_2+N_2	NH_3+O_2+He	NH_3+O_2+Ar/N_2	H_2+N_2O+Ar
Mathieu and Petersen [11]	2015					[11]	[59,60,61,56,62,63,64]
Nakamura et al. [8]	2017	[17,18,19,22]				[11]	[63]
Okafor et al. [6]	2018						
Glarborg et al. [5]	2018	[17,18,19,20,21,22,23,24]				[11]	
Shrestha et al. [58]	2018	[17,18,19,20,22]				[11]	
Otomo et al. [9]	2018	[17,18,19,22]	[23,65,66,67]			[11]	
Li et al. [13]	2019	[17,18,19,20,21,22]	[21,23,65,66,67]			[11]	
Mei et al. [10]	2019	[17,18,19,20,21,22,23,10,24]		[10]		[11]	
Han et al. [12]	2020	[17,18,19,20,21,22,23,10,24]	[21,23]			[11]	
Shrestha et al. [7]	2020	[17,18,19,20,21,22,23,10,24]	[24,21,23,65,66,67,7]	[10,7]	[7]	[11]	
Stagni et al. [14]	2020	[18,10]				[11,68]	
Present mechanism	2021	[17,18,18,20,21,22,23,10,24]	[21,23,24,7]	[10,7]	[7]	[11]	[59,60,56]

published very recently. Moreover, only ignition delays and species concentration in flow reactors were considered for comparison by the authors of [57], who concluded that the models of Glarborg et al. [5] and Shrestha et al. [58] perform the best. It should be noted that the potential impact of surface reactions on the walls of flow reactors introduces an ambiguity in data interpretation as discussed by, e.g. Glarborg et al. [5]. Therefore, experiments on speciation in flow reactors were not considered for model validation in the present study. The experimental data previously used for comparison with the literature mechanisms in the original studies presenting these models are shown in Table 2. Only the mechanisms of Mathieu and Petersen [11], and Nakamura et al. [8] were validated using ignition delays in H_2+N_2O+Ar mixtures, which are relevant to the present study, while practically all models were compared with ignition delays in NH_3+O_2+Ar/N_2 mixtures [11]. It should be noted that all mechanisms considered were validated using other experiments, e.g., species concentration in flow reactors, or flame propagation in NH_3+CH_4 fuel mixtures, which are beyond the scope of the present study. Summarizing, the models of Glarborg et al. [5], Nakamura et al. [8], Stagni et al. [14], and Shrestha et al. [7], which is the latest modification of the model of Shrestha et al. [58] will be tested. One may note that the Glarborg mechanism was not aiming to model ammonia flames, and its performance for the burning velocities of NH_3+air mixtures, seen in Fig. 1 and of NH_3+O_2+N_2 mixtures is not satisfactory as earlier demonstrated by Mei et al. [10]. However, as will be shown in the following, for the NH_3+N_2O+air laminar burning velocities, it nicely reproduces all experimental trends.

4. Results and discussion

4.1. Experimental results

Fig. 3 shows the present measurements of the laminar burning velocities of NH_3+N_2O+air mixtures at 1 atm and 298 K. Fig. 3(a) depicts the data for $x_{N2O} = 0.5$, where the S_L reaches its maximum close to $\phi = 1.0$, similar to the earlier observations in NH_3+N_2O mixtures [44,45,47,48]. Figure 3(b)(c)(d) presents the relationship between S_L and x_{N2O} at fixed equivalence ratios $\phi = 0.6$, 1.0, and 1.4, respectively. Panel 3(b) includes the measurements of Pfahl et al. [19] in NH_3+N_2O+air flames with nitrous oxide content up to 8%, while Panel 3(c) also shows the literature experimental data of stoichiometric NH_3+air flames, i.e., at $x_{N2O} = 0$, which have been introduced in Fig. 1. The experimental results for the NH_3+air mixture scatter within 1 cm/s, the difference is smaller than the symbol size in Fig. 3.

The present experimental dependences of S_L vs. x_{N2O} at the fixed ϕ are remarkably linear in the whole range investigated, however, close to $x_{N2O} = 0$ the trends deviate from linearity. This can also be found in the predictions of five kinetic mechanisms shown in Fig. 3. Among them, the models of Glarborg et al. [5], Nakamura et al. [8], and Stagni et al. [14] show very close performance for $x_{N2O} = 0.5$ (Fig. 3(a)), the latter one is in particularly good agreement with the experimental data in lean mixtures. Predictions of the mechanism of Shrestha et al. [7] are systematically higher at the stoichiometric and lean side with the deviation increasing with increased x_{N2O}. Recalling that the Glarborg mechanism significantly overpredicts the burning velocities of NH_3+air flames, seen in Figs. 1 and 3, one may conclude that the Nakamura and the Stagni mechanisms show the best performance for NH_3+N_2O+air flames over the entire range of x_{N2O}. On the contrary, Model 1 behaves very closely to these two models for NH_3+air flames (Fig. 1), but dramatically diverges from the experimental data shown in Fig. 3 for increased amounts of nitrous oxide in the oxidizer. Hence, the model development and improvement should be based on consideration of a variety of relevant mixtures and types of experiments, such as flame propagation and self-ignition as will be presented below.

4.2. Development of H/N/O kinetic mechanism

4.2.1. Overall approach

The present H/N/O kinetic mechanism has been developed over the years and passed several iterations. Naturally it has started with the construction of the sub-models of N/O reactions to model decomposition of nitrogen oxides [69] and of N/H reactions to model decomposition of ammonia [70], which was later extended by the reactions of N_2H_x species to reproduce hydrazine chemistry [71]. The primary goal of the H/N/O mechanism development was to incorporate it into the detailed kinetic scheme for small hydrocarbons combustion allowing for modeling of NO_x chemistry in flames. Therefore, the focus of the subsequent studies was on the key reactions of NO formation via major and minor routes [72–74], which permitted to refine the rate constant of, e.g., reaction NNH+O=NH+NO [75]. A complete H/N/O kinetic mechanism consisting of 238 reactions was presented and discussed [76] and included in the releases 0.5 and 0.6 of the Konnov mechanism [77]. Although the performance of the latter was much improved, further updates were found necessary. Several N/O rate constants were modified based on the literature survey of Volkov et al. [78]. Moreover, the analysis of the flame structure of H_2 + O_2 + N_2 flames doped with NO or NH_3 suggested the need for the replacement of the products of reaction NH+H_2O=HNO+H_2 into the formation of NH_2OH [79]. Furthermore, a comparison of this model [79] and the model of Mendiara and Glarborg [80] with the structure of ammonia + air flames [81] revealed the room for

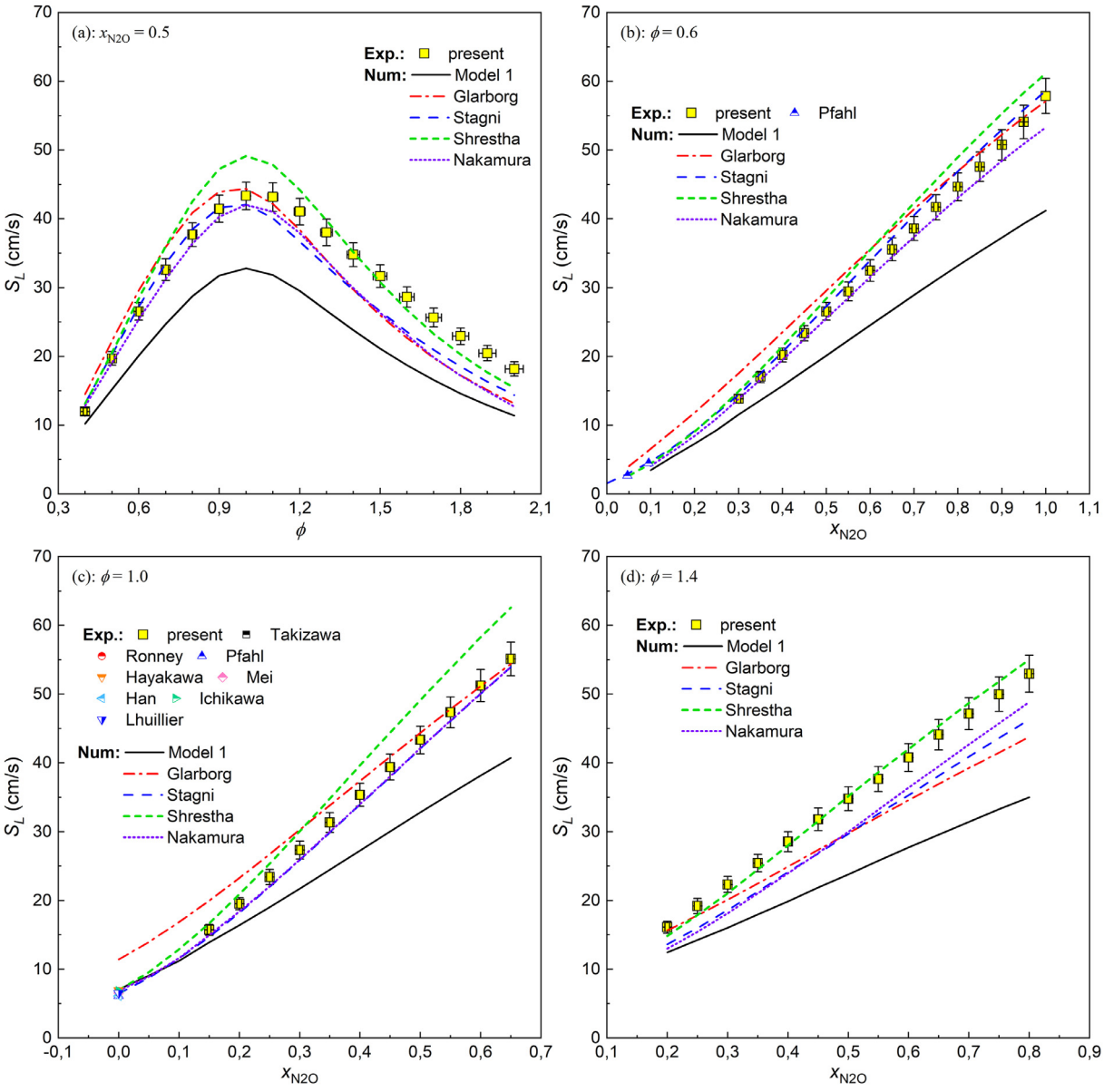

Fig. 3. NH_3+N_2O+air laminar burning velocities at (a): x_{N2O} = 0.5; (b): ϕ = 0.6; (c): ϕ = 1.0; and (d) ϕ = 1.4, at 1 atm and 298 K.

improvement mostly related to the choice of the rate constants. Several updates have been implemented, e.g., the rate constant of reaction N_2+O=NO+N derived by Abian et al. [82], yet in most cases these changes were not properly documented.

The recent version of the detailed kinetic mechanism for small hydrocarbons combustion includes updated H/O kinetic sub-mechanism presented by Konnov [83], and was found in good agreement with the burning velocities and NO_x profiles in flames of propanols [15] and ethylene [84]. In this version, the thermodynamic data for NH, NH_2, NNH, HNO, HONO, HNOH, H_2NO, NH_2OH, NO_3, HNO_3, N_2O_4, N_2H_2, N_2H_3 from the database of Burcat and Ruscic [85] have been implemented. Most recently the rate constant of reaction N_2+O=NO+N was derived in the experimental and kinetic modeling study of NO formation in premixed CH_4+O_2+N_2 flames [16]. Thus, this model of the authors [15,16] (Model 1) was a starting point for the development of the detailed H/N/O kinetic mechanism in the present study. The choice of the rate constants important in the ignition and flame propagation of the mixtures containing NH_3, N_2O, and air is described in the following, while many reactions updated after the publication of the earlier model [76] are outlined in the Supplemental Material. The rate constant expressions in the present model are based on experimental, theoretical or review data and there has been no modification (adjustment or tuning) of the parameters to accommodate experimental results. Rate constants have units of cm^3 mol s and the activation energies are in cal/mol. All reactions considered in the present study are listed in Table 3, and those modified are marked. The new H/N/O mechanism is in the following called Model 2 and is available in the Supplemental Material.

A straightforward approach to elucidate the model deficiencies and improve it is the sensitivity analysis. When normalized reaction sensitivities are largely different for two models at the same conditions, this may indicate that some pathways are suppressed or not included and compensated by other routes, making an agreement with experimental data simply fortuitous. Fig. 4 presents the sensitivity spectra for the burning velocities of NH_3+N_2O+air mixtures with x_{N2O} = 0.5 at ϕ = 0.6, 1.0, and 1.4,

Table 3
Sensitive reactions analyzed in the present study; units are cm^3 mol s cal K, $k = AT^n \exp(-E_a/RT)$, UF = uncertainty factor. * indicates reactions in Model 2 different from Model 1.

No.	Reaction	A	n	E_a	Temperatures	UF	Source Model 2	Source Model 1
1*	$N_2O(+M)=N_2+O(+M)$	9.90E+10	0	57,900	1000–3000	3.2	[86]	[86]
	Low pressure limit:	6.00E+14	0	57,440	1000–3000	2.0	[86]	[86]
	TROE /−0.2 7300.0 10.0 /				1000–3000	1.3	[86,78]	[86,78]
	Enhanced third-body efficiencies (relative to Ar):							
	O_2 = 1.4, N_2 = 1.7, H_2O=12,					1.4	[142]	[142]
	N_2O = 3.5,					2	[89]	[89]
	NO = 3					2	[143]	[143]
2	$N_2O+O = N_2+O_2$	3.69E+12	0	15,940	1075–3340	1.6	[91,86]	[91,86]
3	$N_2O+O=NO+NO$	9.15E+13	0	27,680	1370–4080	1.6	[91,86]	[91,86]
4*	$NH+H = N + H_2$	1.88E+08	1.55	205	300–2000	1.5	[94]	[93]
5*	$NH_2+H=NH+H_2$	1.09E+5	2.59	1812.3	300–2000	1.5	[100]	[95]
6*	$NH_2+NH=N_2H_2+H$	4.26E+14	−0.272	−77.5	200–2500	2	[104]	[103]
7	$NH_3+\mathbf{H}=NH_2+H_2$	6.40E+05	2.390	10,171	490–1780	1.5	[106]	[106]
8*	$NH_2+H(+M)=NH_3(+M)$	1.60E+14	0.0	0	292–533	2	[107]	[107]
	Low pressure limit:	3.60E+22	−1.76	0	292–533	2	[107]	[107]
	TROE /0.5 1E-30 1E30 1E30/							
	Enhanced third-body efficiencies (relative to N_2):							
	Ar =0.7, H_2O =7, N_2O =2,						p.w.	
	CH_4 =2.6, C_2H_6 =4.8, CO_2 =2.8						[108]	[108]
9*	$N_2H_2+H = N_2+H_2+H$	4.82E+08	1.76	739.2	300–2000	2	[100]	[110]
10*	$N_2H_2=NNH+H$	1.80E+40	−8.410	73,353.0	600–2500	5	[113]	[5]
	+	2.60E+40	−8.530	72,886.2				
	PLOG							
11*	$N_2O+H = N_2+OH$	6.44E+07	1.84	13,490.0	500–2500	2	[117]	[115]
12*	$N_2O+H=NH+NO$	7.34E+20	−1.55	36,940.0	500–2500	2	[117]	[115]
13*	$N_2O+H=NNH+O$	2.25E+19	−1.1	48,180.0	500–2500	2	[117]	[115]
14	$N_2O+H=HNNO$	8.00E+24	−4.39	10,530.0	300–1200	3	[115]	[115]
15*	$N_2O+H=OH^*+N_2$	1.60E+14	0.00	50,300.0	1400–2000	2	[118]	–
16*	$N_2O+H_2=N_2+H_2O$	7.00E+12	0	32,500.0	1410–1810	3	[56]	–
17*	$N_2O+OH=N_2+HO_2$	1.30E-2	4.72	36,561.0	1000–5000	3	[121]	[119]
18*	$N_2O+OH=HNO+NO$	1.18E-4	4.33	25,082.0	1000–5000	3	[121]	[120]
19	$NH+N_2O=N_2+HNO$	2.00E+12	0.0	6000.0	1000–3000	5	[122]	[122]
20	$NH+OH=HNO+H$	3.24E+14	−0.376	−45.7	200–2500	2	[104]	[104]
21	$NH+OH=N + H_2O$	1.58E+07	1.737	−576	200–2500	2	[104]	[104]
22	$NH+OH=NO+H_2$	1.62E+13	−0.376	−45.7	200–2500	2	[104], p.w.	[104]
23	$NH_2+O=HNO+H$	6.60E+13	0.0	0	242- 473	1.3	[125]	[125]
24*	$NH_2+O_2=H_2NO+O$	2.62E+11	0.487	29,050	500–2500	2	[117]	[126]
25*	$NH_2+O_2=HNO+OH$	2.88E-02	3.76	18,180	500–2500	2	[117]	[126]
26	$NH_2+NO=N_2+H_2O$	2.61E+19	−2.369	866	400–1900	1.5	[128]	[128]
27	$NH_2+NO=NNH+OH$	4.29E+10	0.294	−870	400–1900	1.5	[128]	[128]
28	$NH_3+OH=NH_2+H_2O$	5.00E+07	1.6	950.0	225–2000	2.5	[123]	[123]
29	$H+NO(+M)=HNO(+M)$	1.52E+15	−0.41	0.0	230–4200	5	[130]	[130]
	Low pressure limit:	2.36E+14	0.206	−1550	295–905	1.5	[133]	[133]
	TROE / 0.82 1.0 1.0E+10 /							
	Enhanced third-body efficiencies (relative to Ar):							
	N_2 =1.6							
30	$HNO+H=NO+H_2$	6.69E+10	0.94	495	200–2500	2	[137]	[137]
31	$HNO+OH=NO+H_2O$	1.20E+09	1.189	334	200–2500	2	[137]	[137]
32*	$HNO+NH_2=NH_3+NO$	5.87E+02	2.950	−3469	550–3000	2	[138]	[4]
33	$NNH+O=NH+NO$	2.00E+14	0.0	4000	1200–2500	2	[73]	[73]
34	$N_2H_2+NO=N_2O+NH_2$	4.00E+12	0.0	11,922	600–2500	5	[113]	[113]

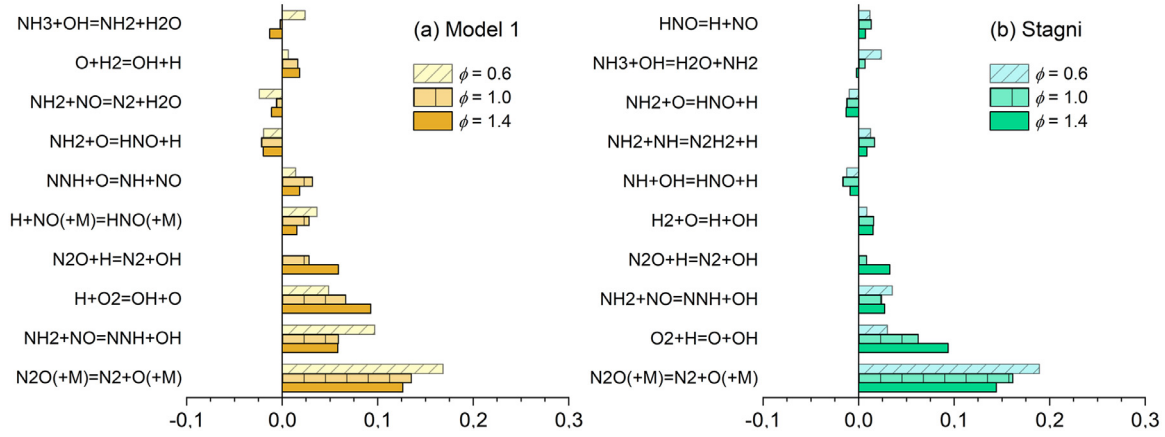

Fig. 4. Normalized A-factor reaction sensitivities of the laminar burning velocities of NH_3+N_2O+air flames with x_{N2O} = 0.5, calculated using (a) Model 1; and (b) the Stagni mechanism.

obtained using Model 1 and the Stagni mechanism [14]. The reaction of nitrous oxide decomposition,

$$N_2O(+M) = N_2+O(+M) \quad (1)$$

has the highest sensitivity in both mechanisms. The rate expressions (high-pressure and low-pressure limiting rate constants) adopted in the Stagni mechanism and Model 1 are both from the review of Baulch et al. [86], however, the auxiliary parameters are not the same. Specifically, the so-called Troe centering $F_{cent} = 1.167–1.25E^{-04}$ T [86] was ignored in the Stagni model, while in Model 1 it was approximated by Volkov et al. [78] as three parameters suitable for the Chemkin interpreter and shown in Table 3. On the other hand, the collisional efficiencies implemented in Model 1 do not include that of H_2O; this omission is explained by the fact that recommendations of Volkov et al. [78] were given for N/O system only. Hence, in Model 2 the enhanced third-body efficiencies for O_2, N_2, N_2O, NO, and H_2O were taken the same as in the original version of the N/O mechanism [69]. Most recently, the rate constants of nitrous oxide decomposition were derived theoretically [87,88] and investigated experimentally in the temperature range of 860–1023 K [88]. In both studies, the authors stated that their calculations are in good agreement with the earlier studies [89,90] which in turn were taken into account by Baulch et al. [86] to derive the recommended expressions, and are, therefore, kept in Model 2.

The addition of the collisional efficiency of H_2O to reaction (1) in Model 2 notably increases the predicted S_L values of NH_3+N_2O+air mixtures, e.g., by 8 cm/s at $x_{N2O} = 0.5$ and $\phi = 1.0$, largely improving agreement with the present experiments. However, further modifications of the H/N/O mechanism will be discussed via a concerted analysis of the kinetic mechanism performance using different experiments. To properly model ignition delay times measured in shock tubes, two reactions previously absent in Model 1 were included: $N_2O+H_2=N_2+H_2O$ and $N_2O+H=OH^*+N_2$ with the rate constants discussed in the following. The first reaction was suggested to be unimportant [56], while the second one is needed to properly model the formation of excited OH radicals often used to register self-ignition in shock-tube experiments.

Figures 5–7 present additional experimental data used for Model 1 validation and sensitivity analysis. Figure 5 shows the laminar burning velocities of NH_3+H_2+air mixtures from Lhuillier et al. [24] and Han et al. [21] and predictions of two models. Figure 6 compares ignition delays in NH_3+O_2+Ar lean, stoichiometric and rich mixtures from Mathieu and Petersen [11] with modeling, while Fig. 7 depicts ignition delay times of N_2O+H_2+Ar mixtures from Mulvihill et al. [56]. Although the behavior of Model 1 can be considered as satisfactory as seen in Figs. 1,5, and 7, further improvement could be achieved via analysis of the most sensitive reactions.

Figure 8 shows the normalized A-factor reaction sensitivities calculated using Model 1 after modifying the rate constant of reaction (1) and incorporation of reactions $N_2O+H_2=N_2+H_2O$ and $N_2O+H=OH^*+N_2$ at the conditions of experimental data shown in Figs. 1,5,6, and 7. Ten most sensitive reactions are presented in each panel, together with the relative difference between the corresponding experimental and simulation results ((Exp.-Num.)/Num.). The error bars shown for the relative difference were propagated from the claimed experimental uncertainties. The laminar burning velocities of NH_3+air and NH_3+H_2+air flames from Han et al. [21] are used in panels (a) and (b), while ignition delay times of NH_3+O_2+Ar and N_2O+H_2+Ar flames, from Mathieu and Petersen [11], and Mulvihill et al. [56], respectively, are used in panels (c) and (d). These relative differences are helpful in the analysis of possible effects of the modification of a specific rate

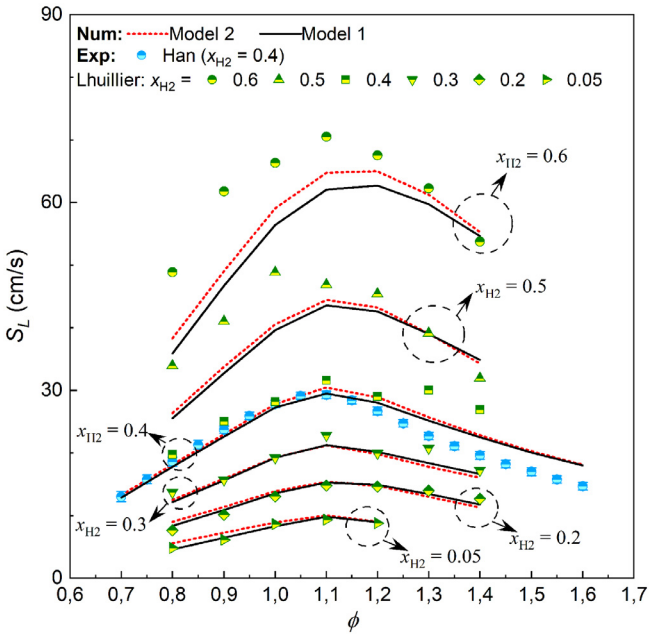

Fig. 5. S_L of NH_3+H_2+air flames with various vol% H_2 in the fuel at room temperature and 1 atm. Symbols: experiments [24,21], lines: modeling.

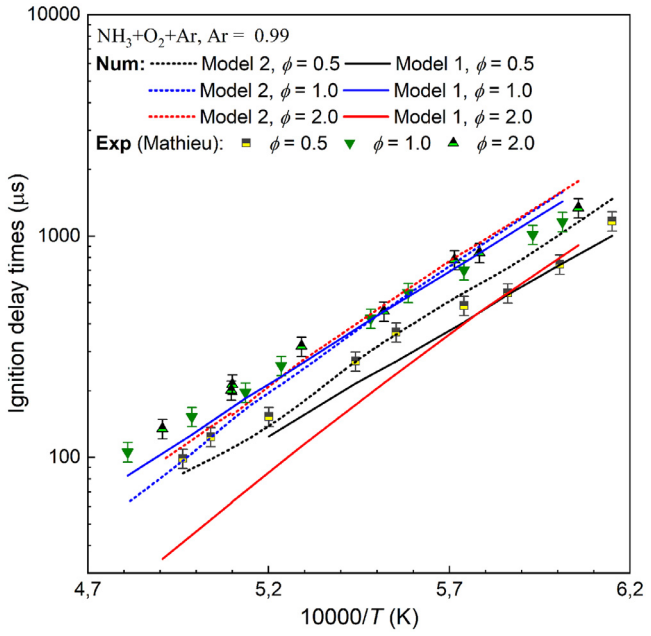

Fig. 6. Ignition delay times of NH_3+O_2+Ar mixtures at 11 atm with 99 vol% Ar dilution. Symbols: experiments [11], lines: modeling. Ignition is defined as the intersection of the tangent to $(dOH^*/dt)_{max}$ with the zero emission line [11].

constant for all experimental conditions used as a reference. All reactions seen in Fig. 4 for NH_3+N_2O+air flames and in Fig. 8 will be discussed in the following, except the H/O reactions presented in the updated hydrogen mechanism [83] and therefore left unchanged.

4.2.2. N/O reactions

Together with reaction (1) discussed above, only reaction

$$N_2O + O = N_2 + O_2 \quad (2)$$

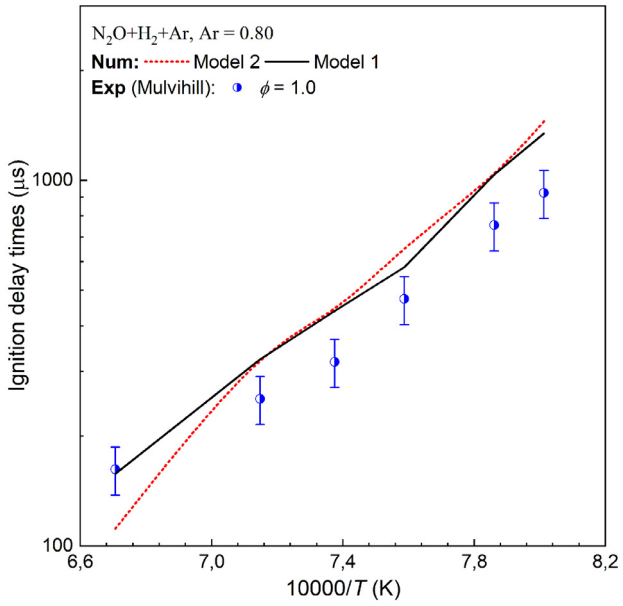

Fig. 7. Ignition delay times of N_2O+H_2+Ar mixtures at 0.69 atm with 80 vol% Ar dilution. Symbols: experiments [56], lines: modeling. Ignition is defined as the intersection of the tangent to $(dOH^*/dt)_{max}$ with the zero emission line [56].

appears in the sensitivity spectra among N/O reactions. Investigations of the rate constant of reaction of nitrous oxide with oxygen atom, which has the second channel

$$N_2O + O = NO + NO \quad (3)$$

and their branching ratio have a long history. In the earlier work devoted to the development of N/O mechanism [69], it was, for example, shown that too-low or too-high values of the rate constants for reactions (2) and (3) are incompatible with experimental data on N_2O decomposition. Later Meagher et al. [91] performed a comprehensive evaluation of the literature pertaining to these reactions. As a result, recommendations for the rate constants of these two reactions were given over wide temperature ranges. These recommendations were supported by Baulch et al. [86] and adopted in various mechanisms including Model 1 and Model 2.

4.2.3. N/H reactions

Reaction

$$NH+H = N + H_2 \quad (4)$$

has a minor impact on the calculated ignition delays in N_2O+H_2+Ar mixtures. In many kinetic models the rate constant of it is taken from the flame study of Morley [92] or from the shock-tube investigation of the reverse reaction by Davidson and Hanson [93], the latter was adopted in Model 1. Since then many theoretical works claimed good agreement with these experiments. Only Adam et al. [94] performed new measurements at room temperature and calculated the rate constant for the range 300–2000 K. Their expression agrees well with all available data [92–94] and was therefore adopted in Model 2.

The rate constant of reaction

$$NH+H_2=NH_2+H \quad (-5)$$

in Model 1 was taken from the shock-tube study of Rohrig and Wagner [95] because it was later supported by the experiments of Fontijn et al. [96] and theoretical calculations of Mackie and Bacskay [97]. Samu et al. [98] attempted optimization of this rate constant using the same experiments [95,96] together with concentration profiles of NH_2 radicals obtained in flames [99]. Their expression, however, disagrees with the most recent high-level theoretical calculations [100] of the reverse reaction. Hence in Model 2, reaction

$$NH_2+H=NH+H_2 \quad (5)$$

replaces the reverse one and the rate constant of Li and Sarathy [100] is adopted.

Kinetic studies of reaction

$$NH_2+NH=N_2H_2+H \quad (6)$$

were limited to room temperature, e.g., [101,102]. At high temperatures, the rate constant was derived from 2200 to 2800 K by fitting the concentration profiles of NH and NH_2 to a complex mechanism by Davidson et al. [103] and their expression was implemented in Model 1. The theoretical calculations of Klippenstein et al. [104] are somewhat higher than available experimental data, nevertheless, they are adopted in Model 2 for consistency since many other calculated rate constants from this work were implemented in both models; these reactions are outlined in the Supplemental Material.

The latest experimental investigations of the rate constant of reaction

$$NH_3+H=NH_2+H_2 \quad (7)$$

have been performed more than 30 years ago by Ko et al. [105] over the temperature range 490–960 K, and by Michael et al. [106] who covered 750–1777 K range. Taking into account other data from the literature, they proposed rate expressions almost identical at high temperatures. Since then only theoretical studies of reaction (7) have been performed often reproducing the experimental results. Most recently Stagni et al. [14] also calculated this rate constant which in their work is about two times higher than the available measurements [105,106]. In both Model 1 and Model 2 the expression of Michael et al. [106] is adopted.

Reaction of ammonia decomposition

$$NH_2+H(+M)=NH_3(+M) \quad (8)$$

has been studied in the literature in both forward and reverse directions. It is mostly sensitive for prediction of ignition delays of ammonia-containing mixtures and then, in the falloff region, depends on the bath gas. Therefore, recent theoretical calculations of the rate constant presented in PLOG format (which does not accommodate third-body efficiencies), e.g., in the mechanism of Stagni et al. [14], can be good for one diluent only. The rate expressions (high-pressure and low-pressure limit rate constants) adopted in Model 1 and Model 2 are from the combined experimental and theoretical study of Altinay and Macdonald [107], who provided them for N_2 as a bath gas. The same authors [108] determined collisional efficiencies for reaction (8) as N_2: CH_4: C_2H_6: CO_2 = 1: 2.6: 4.8: 2.8. In addition, collisional efficiencies were estimated in Model 2 as N_2: Ar: H_2O: N_2O = 1: 0.7: 7: 2. It should be noted that these estimated values could be in reality temperature-dependent [109] and certainly deserve further studies.

There are no experimental rate constants available for the reaction between diazene, N_2H_2, and H atoms. In Model 1 it is included as

$$N_2H_2+H=NNH+H_2$$

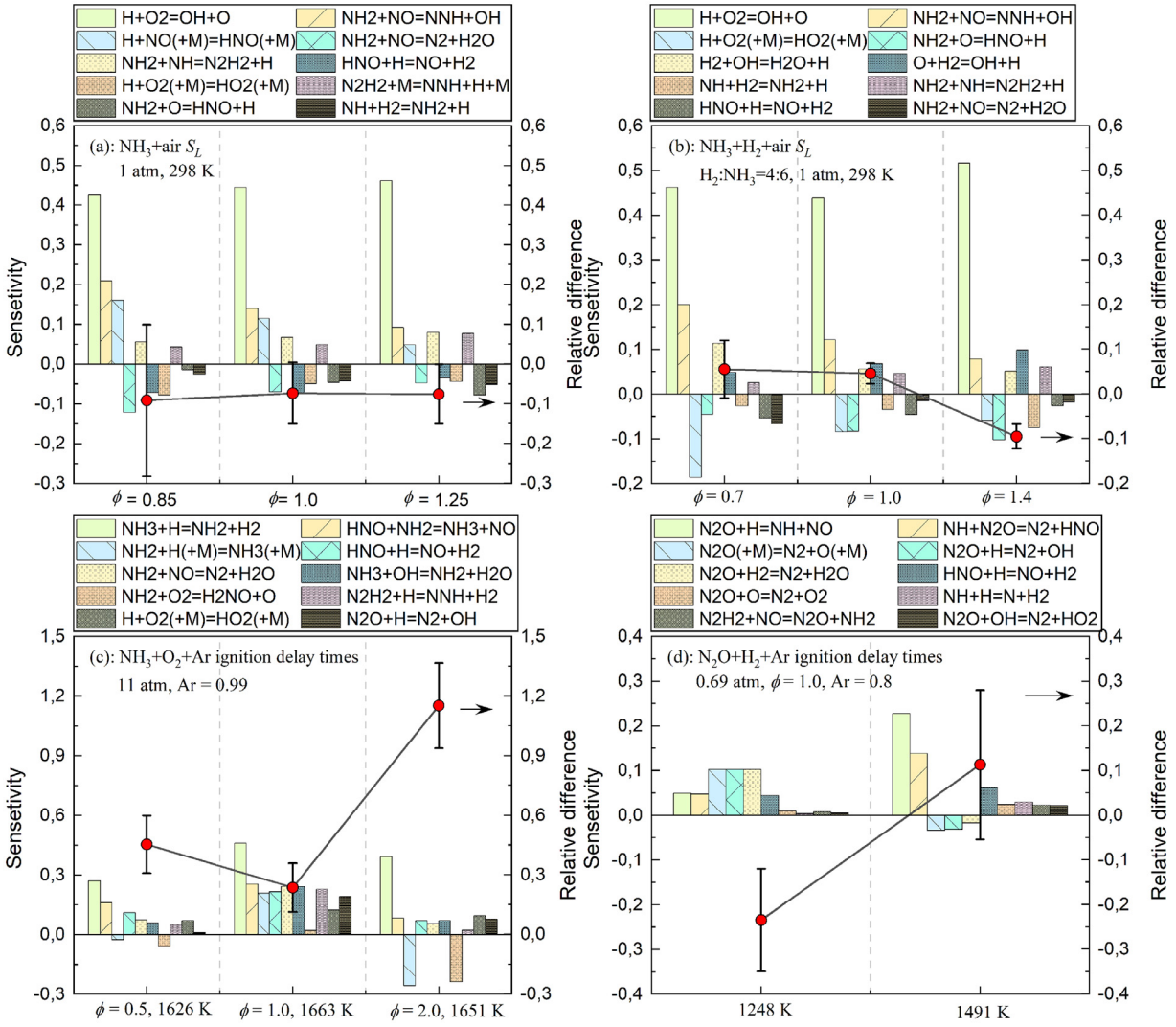

Fig. 8. Normalized A-factor reaction sensitivities and the relative difference between experimental and simulation results, calculated using Model 1. (a): laminar burning velocities of NH_3+air flames at 298 K and 1 atm; (b): laminar burning velocities of NH_3+H_2+air flames at 298 K and 1 atm with 40 vol% H_2 in the total fuel; (c): ignition delay times of NH_3+O_2+Ar mixtures at 11 atm with 99 vol% Ar in the reactants; (d): ignition delay times of stoichiometric N_2O+H_2+Ar mixtures at 0.69 atm with 80 vol% Ar in the reactants.

with the rate constant calculated by Linder et al. [110]. Later Truhlar and co-workers revisited this reaction in several studies and compared results obtained at different levels of theory [111]. Most recently Li and Sarathy [100] implemented larger basis sets compared to previous works and derived the rate constant adopted in Model 2. It should be noted that this rate constant is about an order of magnitude higher than that of Linder et al. [110] and 3–4 times higher than calculations of Zheng et al. [111]. Even more important, Döntgen and Leonhard [112] analyzed this reaction as an example of separation of chemical and relaxation kinetics and found that for diazinyl, hot β-scission fully replaces the sequence of hydrogen abstraction and decomposition of NNH that means that reaction should be written as

$$N_2H_2+H = N_2+H_2+H \quad (9)$$

which is adopted in Model 2.

The reaction of diazene decomposition was in Model 1 presented as a bimolecular process

$$N_2H_2+M=NNH+H + M$$

with the rate constant based on the model of Glarborg et al. [5], but divided by 10. In Model 2 the pressure-dependent rate constant calculated by Dean and Bozzelli [113] for N_2 as a bath gas is adopted. Note that this rate constant was presented as a sum of PLOG functions for reaction

$$N_2H_2=NNH+H \quad (10)$$

while in Table 3 only terms at 1 atm are listed.

4.2.4. H/N/O reactions

One of the most sensitive reactions for the laminar burning velocities of NH_3+N_2O+air flames (Fig. 4) and ignition delay times of N_2O+H_2+Ar mixtures (Fig. 8) is reaction

$$N_2O+H = N_2+OH \quad (11)$$

which converts H atoms to OH radicals. It has other, less important channels

$$N_2O+H=NH+NO \quad (12)$$

$$N_2O+H=NNH+O \quad (13)$$

$$N_2O+H=HNNO \quad (14)$$

$$N_2O+H=OH^*+N_2 \quad (15)$$

The total rate constant of N_2O+H=Products has a distinct behavior with different effective activation energies below and above 750 K, which was attributed by Marshall et al. [114] to the effect of tunneling. In Model 1 the rate constants of reactions (11) – (14) were taken from Bozzelli et al. [115], who concluded that pressure-dependent reaction (14) is responsible for this behavior and calculated its rate constant at 1 atm for N_2 as a bath gas. One may note that the calculated rate constant of reaction (14) at 1 atm for Ar as a bath gas by Diau and Lin [116] is close to that of Bozzelli et al. [115] around 1000 K, but is about 5 times higher at room temperature. In Model 2 the rate constants of reactions (11) – (13) are adopted from the study of Klippenstein et al. [117] who confirmed the analysis of Bozzelli et al. but did not provide the expression for reaction (14) which is thus not changed. Reaction (15) is one of the dominant routes forming OH^* chemiluminescence in the H_2+N_2O shock tube experiments [118], it was added here with the rate constant obtained by Hidaka et al. [118] since many shock tube investigations use the OH^* trace to define ignition delay times.

As is mentioned above, reaction

$$N_2O+H_2=N_2+H_2O \quad (16)$$

was included in Model 2 to verify that it is 'unimportant' as suggested by Mulvihill et al. [56]. Revisiting experimental conditions of the study of Kosarev et al. [62] on ignition delay times in H_2+N_2O mixtures Mulvihill et al. [56] concluded that the reaction rate of reaction (16) should be at least 30 times lower than that suggested before [62]. Nevertheless, with this rate constant, which is adopted in Model 2, reaction (16) appears in the sensitivity spectra at the conditions of experiments of Mulvihill et al. [56] shown in Fig. 8(d) indicating the need for further investigation of this reaction.

Reaction

$$N_2O+OH=N_2+HO_2 \quad (17)$$

has minor sensitivity in calculated ignition delay times for H_2+N_2O mixtures converting OH into less reactive HO_2 radicals. In Model 1 the rate constant of this reaction was taken from the study of Rutar et al. [119], while the second channel was included in reverse direction HNO+NO=N_2O+OH with the rate constant derived by Diau et al. [120]. In Model 2 the rate constants of both reaction (17) and

$$N_2O+OH=HNO+NO \quad (18)$$

are adopted from the theoretical study of Mebel et al. [121].

Reaction

$$NH+N_2O=N_2+HNO \quad (19)$$

was never investigated and only suggested by Hanson and Salimian [122] with estimated rate constant which is adopted in both Model 1 and Model 2.

As seen in the sensitivity spectra for NH_3+N_2O+air flames (Fig. 4), reaction

$$NH+OH=HNO+H \quad (20)$$

appears only for the mechanism of Stagni et al. [14], which implemented rate constants for this and the second channel

$$NH+OH=N + H_2O \quad (21)$$

suggested by Cohen and Westberg [123], who considered only two product channels of reaction between imidogen and hydroxyl radicals. However, theoretical calculations of Sumathi et al. [124] showed that competitive products are to be HNO+H and NO+H_2 with roughly equal branching. In contrast, Klippenstein et al. [104] later obtained different rate constants for reactions (20) and (21), which are adopted in both Model 1 and Model 2. It was also noted [104] that contribution of reaction

$$NH + OH = NO + H_2 \quad (22)$$

is less than 5% compared to HNO+H channel. The rate constant of this reaction was thus taken as 1/20 of that of reaction (20).

Inomata and Washida [125] investigated reaction

$$NH_2+O=HNO+H \quad (23)$$

from 242 to 473 K in 2–7.5 Torr of He and concluded that it has no pressure or temperature dependence, which was later confirmed by the theoretical calculations of Sumathi et al. [124]. The rate constant agrees well with the measurements of Dransfeld et al. [101] and is kept the same in both Model 1 and Model 2.

The rate constants of reaction

$$NH_2+O_2=H_2NO+O \quad (24)$$

and its minor channel

$$NH_2+O_2=HNO+OH \quad (25)$$

were in Model 1 adopted from the experimental study of Hennig et al. [126] who suggested that the channel leading to NO+H_2O could be the main reaction path. The QRRK analysis of Dean and Bozzelli [113] did not reconcile these measurements and predicted much lower rate constants for reactions (24) and (25). Klippenstein et al. [117] repeated theoretical calculations for this system at a higher level of theory and found good agreement with the results of Dean and Bozzelli [113] for reaction (24). Therefore, the rate constants for both channels [117] are adopted in Model 2.

Reactions

$$NH_2+NO=NNH+OH \quad (26)$$

$$NH_2+NO=N_2+H_2O \quad (27)$$

appear in all sensitivity spectra for ammonia flame propagation or ignition. Not only absolute values of their rate constants but also branching ratio affect behavior of the models as discussed by Miller and Glarborg [127] and in many other relevant studies. Contemporary kinetic models for ammonia often implement very close expressions originating from experimental works or theoretical calculations and they all agree within a factor of 2 as noted by Klippenstein et al. [117]. In the mechanisms of Glarborg et al. [5], and Stagni et al. [14] as well as in Model 1 and Model 2 the same rate constants suggested by Song et al. [128] are used.

Similarly, reaction

$$NH_3+OH=NH_2+H_2O \quad (28)$$

has been investigated in many experimental works mostly in 70s and 80s and summarized by Cohen and Westberg [123]. Quantum chemistry calculations performed since then were found with a different degree of agreement with the measurements. For instance, Stagni et al. [14] calculated this rate constant which is about two times higher than the available data [123,42], while the optimized rate constant of Samu et al. [98] is 2–3 times lower at

high temperatures typical for combustion. In both Model 1 and Model 2 the recommendation of Cohen and Westberg [123] is kept, which is strongly supported by the theoretical study of Nguyen and Stanton [129].

Decomposition / recombination reaction

$$H+NO\ (+M) = HNO\ (+M) \quad (29)$$

has been investigated in many works and analyzed by Tsang and Herron [130] and by Baulch et al. [86]. In the latter review, only recommendation for H_2 as a bath gas was provided; moreover, it was noticed that flow reactor studies [131,132] indicate rate constants at high temperatures about a factor of 3–4 lower than being expected from the evaluated expressions [130,86]. Riley et al. [133] determined the rate constants up to 905 K and confirmed that earlier recommendations were too high. Following suggestion of Rasmussen et al. [134] the high-pressure limit rate constant and center broadening parameter from Tsang and Herron [130] are combined with the low-pressure expression and collisional efficiency for N_2 of Riley et al. [133] in Model 1 and Model 2. Stagni et al. [14] calculated this rate constant and found that their expression overestimates available measurements at room temperature.

A comprehensive summary of scattered measurements and earlier theoretical studies [135,136] of reactions

$$HNO+H = NO + H_2 \quad (30)$$

$$HNO+OH = NO + H_2O \quad (31)$$

was provided by Nguyen et al. [137]. They performed canonical and microcanonical variational transition state calculations suggesting that μVT results should be more accurate, which are accepted in Model 1 and Model 2. On the other hand, Nguyen et al. [137] emphasized the need for experimental studies of these reactions since their expressions significantly differ from the calculations of Soto et al. [135,136], which are often adopted in combustion mechanisms.

In the absence of experimental data for reaction

$$HNO+NH_2=NH_3+NO \quad (32)$$

the estimation by Miller and Bowman [4] was used in Model 1. Ab initio calculations of Xu and Lin [138] are somewhat lower than the earlier results of Mebel et al. [139], which was explained by the more accurate determination of the potential energy surface. The rate constant of Xu and Lin [138] is adopted in Model 2 as well as in the mechanism of Glarborg et al. [5].

The rate constants of the remaining reactions that appeared in the sensitivity spectra have not been changed. Reaction

$$NNH+O=NH+NO \quad (33)$$

as a possible new route for NO formation in flames was first discussed by Bozzelli and Dean [140], who suggested negative activation energy for its rate constant. Konnov and De Ruyck [73] attempted to derive this rate constant from experimental data on NO formation in low-pressure flames with positive activation energy of 4 kcal/mol. The theoretical calculations of Haworth et al. [141] appeared much lower than the rate of Bozzelli and Dean [140] with very modest temperature dependence, while those of Klippenstein et al. [117] confirmed these observations. The rate constant of this reaction [73] is kept the same in Model 1 and Model 2 since its update requires revisiting of NO predictions in hydrogen and syngas flames, which is beyond the scope of the present work.

The rate constant of reaction

$$N_2H_2+NO=N_2O+NH_2 \quad (34)$$

was estimated by Dean and Bozzelli [113] and apparently has not received further attention since then. Other reactions updated after the publication of the earlier H/N/O model [76] and kept the same in Model 1 and Model 2 are outlined in the Supplemental Material.

4.3. Model performance

4.3.1. Burning velocities

Predictions of the updated Model 2 are compared with the present experimental data in Fig. 9. For NH_3+N_2O+air flames with $x_{N2O} = 0.5$ the mechanism closely reproduces burning velocities in lean mixtures, while in rich mixtures the underprediction is significant. Model 2 performance at these conditions is similar to that of Nakamura et al. [8] and Stagni et al. [14] mechanisms, depicted in Fig. 3. At higher mixing ratios x_{N2O}, the deviation increases, yet the agreement of Model 2 with the present data is improved compared to Model 1.

For $NH_3+O_2+N_2$ flames of different compositions and at different conditions, Model 2 shows very close performance to Model 1 in rich mixtures, while slightly overestimates burning velocities in lean mixtures. The comparison with the literature data presented in Fig. 1 for the laminar burning velocities of NH_3+air flames at 1 atm and 298 K is shown in Fig. S1 in the Supplemental Material. Similar behavior of the two models is seen in comparison with the measurements performed by Hayakawa et al. [22] for the same mixtures but at 3 and 5 atm illustrated in Fig. S2. $NH_3+O_2+N_2$ flames with an increased amount of oxygen in the oxidizer have been studied by Shrestha et al. [7] at room and elevated temperature and by Mei et al. [10] at atmospheric and higher pressures. These experiments are compared with predictions of the two models in Fig. S3 and S4, respectively.

Burning velocities of NH_3+H_2+air mixtures have been investigated in several studies mentioned above. Figure 5 compares predictions of Model 1 and Model 2 with the measurements of Lhuillier et al. [24] and Han et al. [21], while Fig. 10 presents experimental data of Ichikawa et al. [144] obtained in stoichiometric NH_3+H_2+air mixtures at 298 K at elevated pressures. An additional example of the behavior of two models at the conditions of experiments of Lhuillier et al. [145] and Shrestha et al. [7] is shown in Fig. S5. In all cases, Model 1 and Model 2 predict burning velocities close to each other.

Although ammonia flames supported by nitric oxide were not considered as a target in the present work, the measurements in NH_3+NO mixtures at 1 atm and 298 K from Checkel et al. [33] and Parker and Wolfhard [34] were compared with Model 1 and Model 2 predictions as shown in Fig. 11. The calculated burning velocities of these flames are highly sensitive to reactions (26) and (27) between NH_2 and NO as illustrated in Fig. 2, and very good agreement of the modeling with experimental data over the entire range of equivalence ratios does not indicate the need for revision of their rate constants. However, recent measurements in rich flames of NH_3+(50%NO+50%N_2) mixtures at 1 atm and 298 K by Mei et al. [35] are not so nicely reproduced by the two models, see Fig. S6. Remarkably, from seven kinetic mechanisms tested in that study [35], none was successful in predicting these experimental data.

4.3.2. Ignition delays

Ignition delay times of NH_3+O_2+Ar mixtures with 99 vol% Ar dilution measured by Mathieu and Petersen [11] were used for validation of many kinetic schemes listed in Table 2. Their experimental data at 11 atm are shown in Fig. 6, while at 1.4 atm and 29 atm are presented in the Supplemental Material, see Fig. S7. At all conditions Model 2 demonstrates highly improved agreement with these measurements compared to Model 1, especially seen for rich mixtures.

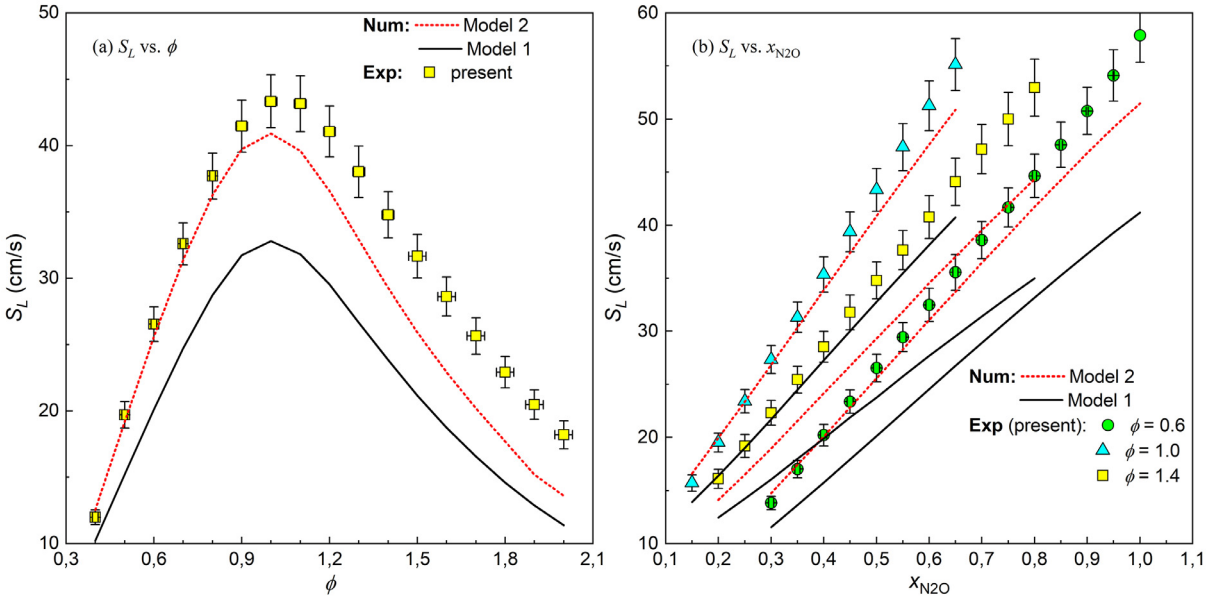

Fig. 9. Predictions of laminar burning velocities at 1 atm using Model 1 and Model 2. Panel (a): S_L as a function of ϕ for NH_3+N_2O+air flames with x_{N2O} = 0.5; Panel (b): S_L as a function of x_{N2O} for NH_3+N_2O+air flames at ϕ = 0.6, 1.0, and 1.4.

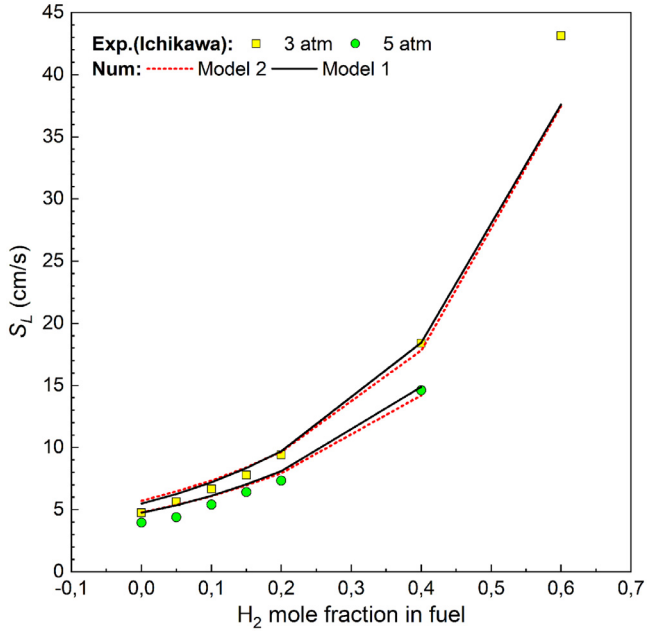

Fig. 10. Predictions of laminar burning velocities using Model 1 and Model 2 for stoichiometric NH_3+H_2+air mixtures at 298 K. Experimental data from Ichikawa et al. [144].

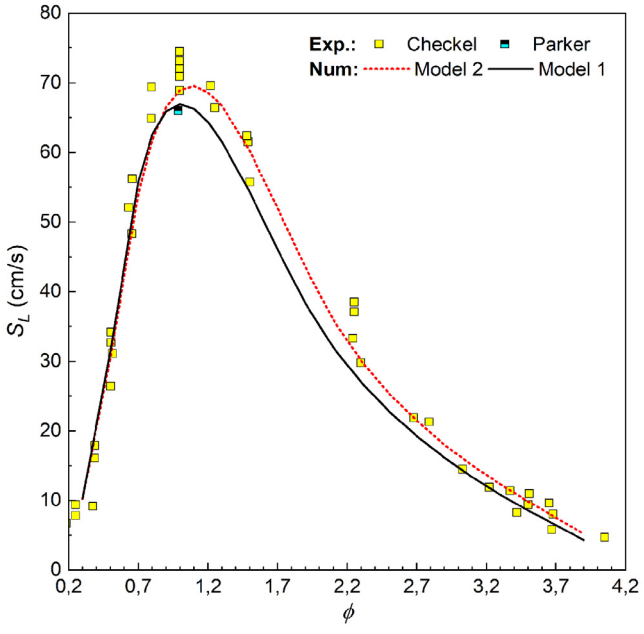

Fig. 11. Predictions of laminar burning velocities using Model 1 and Model 2 for NH_3+NO mixtures at 1 atm and 298 K. Experimental data from Checkel et al. [33] and Parker and Wolfhard [34].

Ignition delay times of N_2O+H_2+Ar mixtures obtained by Mulvihill et al. [56] were also considered for model validation and analysis. Figure 7 shows that Model 1 is actually in satisfactory agreement with these experimental data, while the behavior of the updated Model 2 is very close to it. The situation is different when both models are compared with experimental data from Mevel et al. [59,60] as presented in Fig. 12. In lean, stoichiometric and rich mixtures Model 2 predicts shorter ignition delays and closely matches the measurements particularly at higher pressures.

Summarizing performance of Model 2 achieved after analysis of the sensitive reactions and revision of their rate constants where necessary, one may note that perfect agreement with the new experimental data for NH_3+N_2O+air flames and with the literature data for other ammonia flames and ignition of related mixtures has not been accomplished. The first reason is that selection of the updated rate constants was not aimed at a perfect match with experiment; rather it was guided by a new kinetic knowledge (when available) based on experimentally and theoretically derived rate constants. Following this approach, the rate constants obtained via optimization of kinetic models for a better agreement with the measurements were most often ignored and not incorporated in the present mechanism. The second reason, which is also a common problem for many kinetic models developed for ammonia combustion, is the very limited choice of the available rate

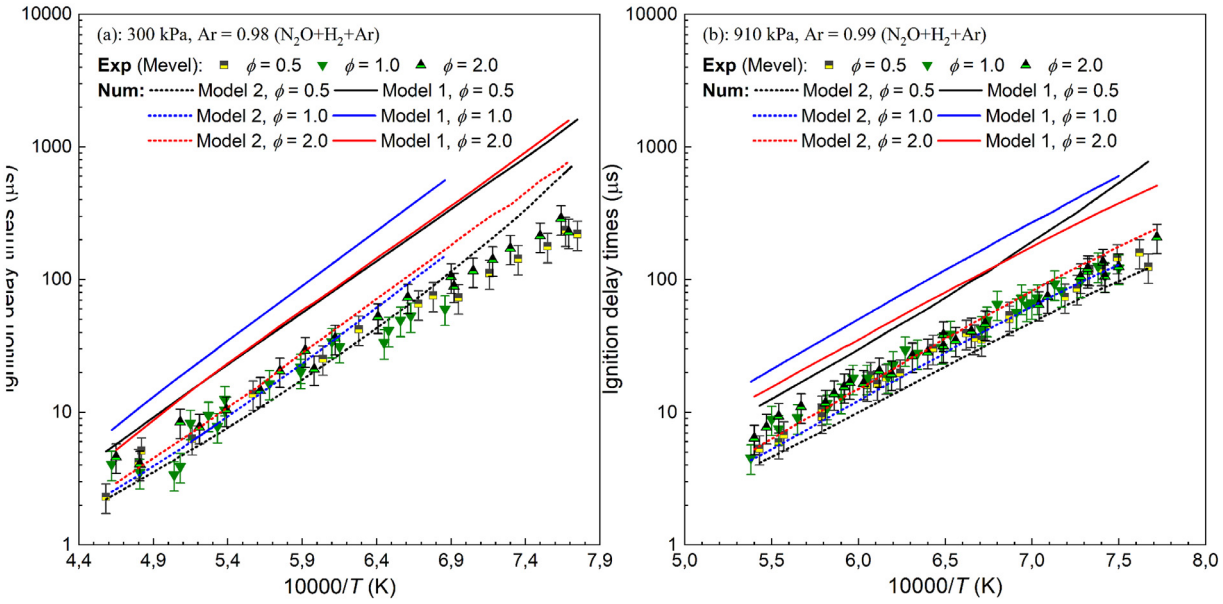

Fig. 12. Predictions of ignition delay times using Model 1 and Model 2 for N_2O+H_2+Ar mixtures. (a) dilution by Ar = 0.98 at 300 kPa [59], (b) dilution by Ar = 0.99 at 910 kPa [60]. Ignition is defined where the OH* reaches 50% of its maximum height [59,60].

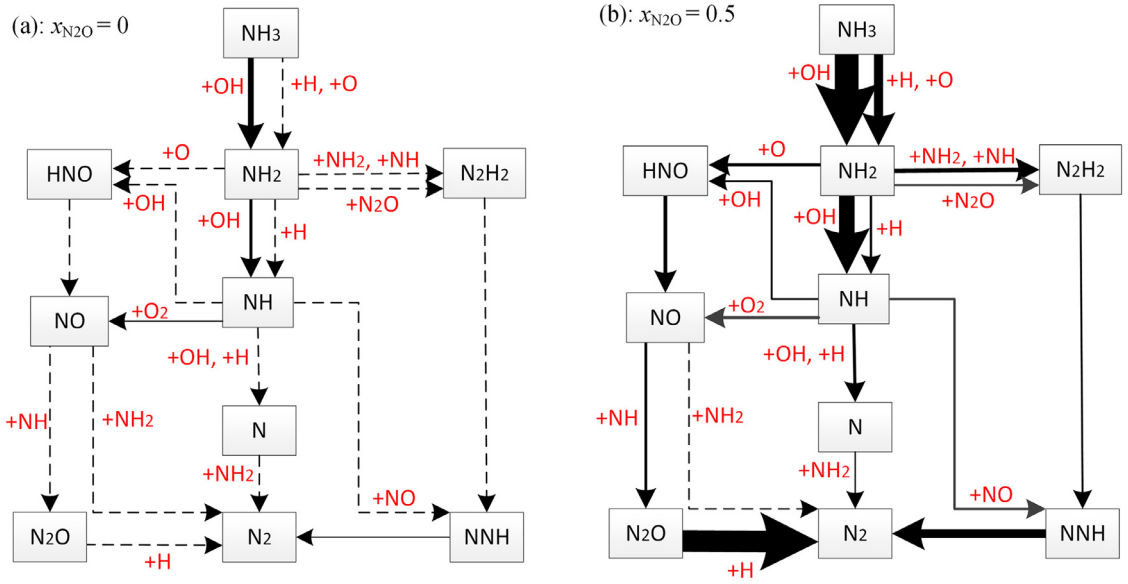

Fig. 13. Reaction pathways of stoichiometric NH_3 oxidation in (a) air; and (b) 50% N_2O + 50% air, calculated using Model 2.

constants for a major part of reactions involved. Frequently recent theoretical calculations are preferred and considered to be most reliable simply because of lack of experimental kinetic studies. Consequently, contemporary kinetic mechanisms often share the same rate constants and demonstrate close performance seldom in a simultaneously good agreement with a range of experimental data available.

4.4. Reaction pathway analysis

The burning velocities of NH_3+N_2O+air flames provide an important independent target for validation and development of detailed kinetic models. This may not be so obvious from the sensitivity spectra shown in Fig. 2, but clearly seen from a comparative reaction pathway analysis for NH_3+N_2O+air and NH_3+air flames. Figure 13 shows reaction pathway analyses for the stoichiometric oxidation processes of NH_3 in air and in N_2O+air with x_{N2O} = 0.5 environments, which were computed using the updated Model 2. Following the approach used for other ammonia flames [12,21], the thickness of the arrows in Fig. 13 represents the integrated rate of species production after being normalized by that of reaction H + O_2 = OH + O at each condition, and the dashed lines denote some reactions with a slightly lower rate of productions. In both panels (a) and (b), the NH_3 consumption mainly occurs in its reaction with OH radical (NH_3+OH=NH_2+H_2O), forming NH_2; and the following oxidation processes share very similar reaction routes. However, most arrows in panel (b) are much thicker than the corresponding arrows in panel (a), which results from substituting part of the air with N_2O. This is also reflected in notably reduced normalized sensitivity of the chain branching reaction H + O_2 = OH + O seen in Fig. 2. From panel (b), nitrous oxide in the x_{N2O} = 0.5 flame reacts predominantly with H radicals through the reaction N_2O+H = N_2+OH (11), and the large amount of OH radicals formed by reaction (11) accelerates the NH_3->NH_2

conversion. When x_{N2O} increases, more OH radicals are released by reaction (11), which can explain why the laminar burning velocity grows rapidly and linearly with the increasing x_{N2O} in Fig. 3.

5. Conclusions

In the present work, the laminar burning velocities of the NH_3+N_2O+air flames were measured using the heat flux method at 1 atm and 298 K, with varied compositions. These experimental data provide an important independent target for the validation and development of detailed kinetic models. Several recently published mechanisms for NH_3 combustion were compared with the new measurements and demonstrated mixed performance. The models of Nakamura et al. [8], and Stagni et al. [14] are in the best agreement simultaneously with the burning velocities of NH_3+air and NH_3+N_2O+air flames over the entire range of the mixing ratios. To improve the H/N/O kinetic mechanism of the authors, the most sensitive reactions in ammonia flame propagation and self-ignition of NH_3+O_2 and H_2+N_2O mixtures were determined and their rate constants were updated when improved kinetic information was available. The choice of the new rate constants is outlined, however, no modification (adjustment or tuning) of the rate parameters to accommodate experimental results was attempted. The updated mechanism demonstrates significantly improved agreement with all measurements used for the model development and with other experimental data from the literature for ammonia flames and self-ignition. The laminar burning velocity of the NH_3+N_2O+air flames has an approximately linear relationship against the fraction of nitrous oxide in the oxidizer mixture, regardless of the tested equivalence ratios. A comparative reaction path analysis for NH_3+N_2O+air and NH_3+air flames revealed that this trend originates from the rate controlling reaction N_2O+H = N_2+OH, which produces OH radicals dominating ammonia oxidation.

Declaration of Competing Interest

The authors declare that they have no known competing financial interests or personal relationships that could have appeared to influence the work reported in this paper.

Acknowledgments

This work was supported by the Knut and Alice Wallenberg Foundation through grant KAW2019.0084 COCALD, the National Scholarship for Building High Level Universities (China Scholarship Council) and State Key Laboratory of Clean Energy Utilization (Project ZJUCEU2019001).

Supplementary materials

Supplementary material associated with this article can be found, in the online version, at doi:10.1016/j.combustflame.2021.01.027.

References

[1] P. Dimitriou, R. Javaid, A review of ammonia as a compression ignition engine fuel, Int. J. Hydrogen Energy 45 (2020) 7098–7118.
[2] H. Kobayashi, A. Hayakawa, K.D. Kunkuma, A. Somarathne, E.C. Okafor, Science and technology of ammonia combustion, Proc. Combust. Inst. 37 (2019) 109–133.
[3] A. Valera-Medina, H. Xiao, M. Owen-Jones, W.I.F. David, P.J. Bowen, Ammonia for power, Prog. Energy Combust. Sci. 69 (2018) 63–102.
[4] J.A. Miller, C.T. Bowman, Mechanism and modeling of nitrogen chemistry in combustion, Prog. Energy Combust. Sci. 15 (1989) 287–338.
[5] P. Glarborg, J.A. Miller, B. Ruscic, S.J. Klippenstein, Modeling nitrogen chemistry in combustion, Prog. Energy Combust. Sci. 67 (2018) 31–68.
[6] E.C. Okafor, Y. Naito, S. Colson, A. Ichikawa, T. Kudo, A. Hayakawa, H. Kobayashi, Experimental and numerical study of the laminar burning velocity of CH_4–NH_3–air premixed flames, Combust. Flame 187 (2018) 185–198.
[7] K.P. Shrestha, C. Lhuillier, A.A. Barbosa, P. Brequigny, F. Contino, C. Mounaïm-Rousselle, L. Seidel, F. Mauss, An experimental and modeling study of ammonia with enriched oxygen content and ammonia/hydrogen laminar flame speed at elevated pressure and temperature, Proc. Combust. Inst. (2020), doi:10.1016/j.proci.2020.06.197.
[8] H. Nakamura, S. Hasegawa, T. Tezuka, Kinetic modeling of ammonia/air weak flames in a micro flow reactor with a controlled temperature profile, Combust. Flame 185 (2017) 16–27.
[9] J. Otomo, M. Koshi, T. Mitsumori, H. Iwasaki, K. Yamada, Chemical kinetic modeling of ammonia oxidation with improved reaction mechanism for ammonia/air and ammonia/hydrogen/air combustion, Int. J. Hydrogen Energy 43 (2018) 3004–3014.
[10] B. Mei, X. Zhang, S. Ma, M. Cui, H. Guo, Z. Cao, Y. Li, Experimental and kinetic modeling investigation on the laminar flame propagation of ammonia under oxygen enrichment and elevated pressure conditions, Combust. Flame 210 (2019) 236–246.
[11] O. Mathieu, E.L. Petersen, Experimental and modeling study on the high-temperature oxidation of ammonia and related NOx chemistry, Combust. Flame 162 (2015) 554–570.
[12] X. Han, Z. Wang, Y. He, Y. Zhu, K. Cen, Experimental and kinetic modeling study of laminar burning velocities of NH_3/syngas/air premixed flames, Combust. Flame 213 (2020) 1–13.
[13] R. Li, A.A. Konnov, G. He, F. Qin, D. Zhang, Chemical mechanism development and reduction for combustion of NH_3/H_2/CH_4 mixtures, Fuel 257 (2019) 116059.
[14] A. Stagni, C. Cavallotti, S. Arunthanayothin, Y. Song, O. Herbinet, F. Battin-Leclerc, T. Faravelli, An experimental, theoretical and kinetic-modeling study of the gas-phase oxidation of ammonia, React. Chem. Eng. 5 (2020) 696–711.
[15] G. Capriolo, C. Brackmann, M. Lubrano Lavadera, T. Methling, A.A. Konnov, An experimental and kinetic modelling study on nitric oxide formation in premixed C_3 alcohols flames, Proc. Combust. Inst. 38 (2021) 805–812, doi:10.1016/j.proci.2020.07.051.
[16] X. Han, M. Lubrano Lavadera, C. Brackmann, Z. Wang, Y. He, A.A. Konnov, Experimental and kinetic modeling study of NO formation in premixed CH_4+O_2+N_2 flames, Combust. Flame 223 (2021) 349–360.
[17] K. Takizawa, A. Takahashi, K. Tokuhashi, S. Kondo, A. Sekiya, Burning velocity measurements of nitrogen-containing compounds, J. Hazard. Mater. 155 (2008) 144–152.
[18] P.D. Ronney, Effect of chemistry and transport properties on near-limit flames at microgravity, Combust. Sci. Technol. 59 (1988) 123–141.
[19] U.J. Pfahl, M.C. Ross, J.E. Shepherd, K.O. Pasamehmetoglu, C. Unal, Flammability limits, ignition energy, and flame speeds in H_2–CH_4–NH_3–N_2O–O_2–N_2 mixtures, Combust. Flame 123 (2000) 140–158.
[20] T. Jabbour, D.F. Clodic, J. Terry, S. Kondo, Burning velocity and refrigerant flammability classification, ASHRAE Trans. 110 (2004) 522–533.
[21] X. Han, Z. Wang, M. Costa, Z. Sun, Y. He, K. Cen, Experimental and kinetic modeling study of laminar burning velocities of NH_3/air, NH_3/H_2/air, NH_3/CO/air and NH_3/CH_4/air premixed flames, Combust. Flame 206 (2019) 214–226.
[22] A. Hayakawa, T. Goto, R. Mimoto, Y. Arakawa, T. Kudo, H. Kobayashi, Laminar burning velocity and Markstein length of ammonia/air premixed flames at various pressures, Fuel 159 (2015) 98–106.
[23] A. Ichikawa, A. Hayakawa, Y. Kitagawa, K.K.A. Somarathne, T. Kudo, H. Kobayashi, Laminar burning velocity and Markstein length of ammonia/hydrogen/air premixed flames at elevated pressures, Int. J. Hydrogen Energy 40 (2015) 9570–9578.
[24] C. Lhuillier, P. Brequigny, F. Contino, C. Mounaïm-Rousselle, Experimental study on ammonia/hydrogen/air combustion in spark ignition engine conditions, Fuel 269 (2020) 117448.
[25] A.A. Konnov, A. Mohammad, V. Ratna Kishore, N. Il Kim, C. Prathap, S. Kumar, A comprehensive review of measurements and data analysis of laminar burning velocities for various fuel+ air mixtures, Prog. Energy Combust. Sci. 68 (2018) 197–267.
[26] E.C. Okafor, Y. Naito, S. Colson, A. Ichikawa, T. Kudo, A. Hayakawa, H. Kobayashi, Measurement and modelling of the laminar burning velocity of methane-ammonia-air flames at high pressures using a reduced reaction mechanism, Combust. Flame 204 (2019) 162–175.
[27] S. Liu, C. Zou, Y. Song, S. Cheng, Q. Lin, Experimental and numerical study of laminar flame speeds of CH_4/NH_3 mixtures under oxy-fuel combustion, Energy 175 (2019) 250–258.
[28] B. Mei, S. Ma, Y. Zhang, X. Zhang, W. Li, Y. Li, Exploration on laminar flame propagation of ammonia and syngas mixtures up to 10 atm, Combust. Flame 220 (2020) 368–377.
[29] S. Wang, Z. Wang, A.M. Elbaz, X. Han, Y. He, M. Costa, A.A. Konnov, W.L. Roberts, Experimental study and kinetic analysis of the laminar burning velocity of NH_3/syngas/air, NH_3/CO/air and NH_3/H_2/air premixed flames at elevated pressures, Combust. Flame 221 (2020) 270–287.
[30] L. Cohen, Burning velocities of ammonia in air and in oxygen, Fuel 34 (1955) S123–S127.
[31] X. Han, Z. Wang, Y. He, Y. Liu, Y. Zhu, A.A. Konnov, The temperature dependence of the laminar burning velocity and superadiabatic flame temperature phenomenon for NH_3/air flames, Combust Flame 217 (2020) 314–320.
[32] Q. Liu, X. Chen, J. Huang, Y. Shen, Y. Zhang, Z. Liu, The characteristics of

flame propagation in ammonia/oxygen mixtures, J. Hazard. Mater. 363 (2019) 187–196.
[33] M.D. Checkel, D.S.K. Ting, W.K. Bushe, Flammability limits and burning velocities of ammonia/nitric oxide mixtures, J. Loss Prev. Process Ind. 8 (1995) 215–220.
[34] W.G. Parker, H.G. Wolfhard, Some characteristics of flames supported by NO and NO_2, Symp. (Int.) Combust. 4 (1953) 420–428.
[35] B. Mei, S. Ma, X. Zhang, Y. Y.Li, Characterizing ammonia and nitric oxide interaction with outwardly propagating spherical flame method, Proc. Combust. Inst. (2020), doi:10.1016/j.proci.2020.07.133.
[36] L.J. Drummond, S.W. Hiscock, Shock-initiated exothermic reactions. II. The oxidation of ammonia, Aust. J. Chem. 20 (1967) 825–836.
[37] L.J. Drummond, Comments upon shock-initiated oxidations by nitrous oxide, Combust. Sci. Technol. 5 (1972) 183–185.
[38] V.M. Zamansky, A.A. Borisov, Mechanism and Promotion of self-ignition of alternative fuels, VINITI Publ., Moscow, 1989.
[39] V.M. Zamansky, A.A. Borisov, Promotion of high-temperature self-ignition, Prog. Energy Combust. Sci. 18 (1992) 297–325.
[40] Y.-y Li, R.-p Jiang, Z.-p Li, S. Xu, F. Pan, L.-f Xie, Studies on the flame propagation characteristic and thermal hazard of the premixed N_2O/fuel mixtures, Def. Technol. 16 (2020) 564–570.
[41] S. Salimian, R.K. Hanson, C.H. Kruger, Ammonia oxidation in shock-heated NH_3-N_2O-Ar mixtures, Combust. Flame 56 (1984) 83–95.
[42] N. Fujii, S. Uchida, H. Sato, S. Fujimoto, H. Miyama, High-temperature reaction of NH_3–N_2O system in shock waves, Bull. Chem. Soc. Jpn. 59 (1986) 3431–3437.
[43] D.T. Venizelos, R.C. Sausa, Detailed chemical kinetics studies of an NH_3/N_2O/Ar flame by laser-induced fluorescence, mass spectrometry, and modeling, Proc. Combust. Inst. 28 (2000) 2411–2418.
[44] P. Ausloos, A. Van Tiggelen, Vitesse de propagation de la flamme dans des mélanges gazeux contenant de l'ammoniac, Bull. Soc. Chim. Belg. 60 (1951) 433–445.
[45] J. Van Wonterghem, A. Van Tiggelen, A., Flame propagation in gaseous mixtures containing nitrous-oxide as oxidant, Bull. Soc. Chim. Belg. 64 (1955) 780–797.
[46] A. Van Tiggelen, J. Deckers, Chain branching and flame propagation, Symp. (Int.) Combust. 6 (1957) 61–66.
[47] D.G.R. Andrews, P. Gray, Combustion of ammonia supported by oxygen, nitrous oxide or nitric oxide: laminar flame propagation at low pressures in binary mixtures, Combust. Flame 8 (1964) 113–126.
[48] J.W. Armjtage, P. Gray, Flame speeds and flammability limits in the combustion of ammonia: ternary mixtures with hydrogen, nitric oxide, nitrous oxide or oxygen, Combust. Flame 9 (1965) 173–184.
[49] P. Gray, R. Mackinven, D.B. Smith, Combustion of hydrogen and oxygen with ammonia and nitrous oxide—Laminar flame speeds and flammability limits at low pressure for ternary mixtures, Combust. Flame 11 (1967) 109–119.
[50] M.J. Brown, D.B. Smith, Aspects of nitrogen flame chemistry revealed by burning velocity modelling, Symp. (Int.) Combust. 25 (1994) 1011–1018.
[51] V.A. Alekseev, J.D. Naucler, M. Christensen, E.J.K. Nilsson, E.N. Volkov, L.P.H. de Goey, A.A. Konnov, Experimental uncertainties of the heat flux method for measuring burning velocities, Combust. Sci. Technol. 188 (2016) 853–894.
[52] M. Lubrano Lavadera, X. Han, A.A. Konnov, Comparative effect of ammonia addition on the laminar burning velocities of methane, n-heptane and iso-octane, Energy Fuels (2020), doi:10.1021/acs.energyfuels.0c03424.
[53] C. Brackmann, T. Methling, M. Lubrano Lavadera, G. Capriolo, A.A. Konnov, Experimental and modeling study of nitric oxide formation in premixed methanol + air flames, Combust. Flame 213 (2020) 322–330.
[54] CHEMKIN-PRO 17.0 (15151), ANSYS reaction design: san diego (2016).
[55] H. Nakamura, M. Shindo, Effects of radiation heat loss on laminar premixed ammonia/air flames, Proc. Combust. Inst. 37 (2019) 1741–1748.
[56] C.R. Mulvihill, O. Mathieu, E.L. Petersen, The unimportance of the reaction $H_2 + N_2O$ $H_2O + N_2$: a shock-tube study using H_2O time histories and ignition delay times, Combust. Flame 196 (2018) 478–486.
[57] L. Kawka, G. Juhász, M. Papp, T. Nagy, I.G. Zsély, T. Turányi, Comparison of detailed reaction mechanisms for homogeneous ammonia combustion, Z. Phys. Chem. 234 (2020) 1329–1357.
[58] K.P. Shrestha, L. Seidel, T. Zeuch, F. Mauss, Detailed kinetic mechanism for the oxidation of ammonia including the formation and reduction of nitrogen oxides, Energy Fuels 32 (2018) 10202–10217.
[59] R. Mével, S. Javoy, F. Lafosse, N. Chaumeix, G. Dupré, C.-.E. Paillard, Hydrogen–nitrous oxide delay times: shock tube experimental study and kinetic modelling, Proc. Combust. Inst. 32 (2009) 359–366.
[60] R. Mével, F. Lafosse, L. Catoire, N. Chaumeix, G. Dupré, C.-.E. Paillard, Induction delay times and detonation cell size prediction of hydrogen-nitrous oxide-diluent mixtures, Combust. Sci. Technol. 180 (2008) 1858–1875.
[61] R. Mével, S. Pichon, L. Catoire, N. Chaumeix, C.-.E. Paillard, J.E. Shepherd, Dynamics of excited hydroxyl radicals in hydrogen-based mixtures behind reflected shock waves, Proc. Combust. Inst. 34 (2013) 677–684.
[62] I.N. Kosarev, S.M. Starikovskaia, A.Y. Starikovskii, The kinetics of autoignition of rich N_2O–H_2–O_2–Ar mixtures at high temperatures, Combust. Flame 151 (2007) 61–73.
[63] O. Mathieu, A. Levacque, E.L. Petersen, Effects of N_2O addition on the ignition of H_2–O_2 mixtures: experimental and detailed kinetic modeling study, Int. J. Hydrogen Energy 37 (2012) 15393–15405.
[64] Y. Hidaka, H. Takuma, M. Suga, Shock-tube studies of N_2O decomposition and N_2O–H_2 reaction, Bull. Chem. Soc. Jpn. 58 (1985) 2911–2916.
[65] P. Kumar, T.R. Meyer, Experimental and modeling study of chemical-kinetics mechanisms for H_2–NH_3–air mixtures in laminar premixed jet flames, Fuel 108 (2013) 166–176.
[66] J. Li, H. Huang, N. Kobayashi, Z. He, Y. Nagai, Study on using hydrogen and ammonia as fuels: combustion characteristics and NO_x formation, Int. J. Energy Res. 38 (2014) 1214–1223.
[67] J. Lee, J. Kim, J. Park, O. Kwon, Studies on properties of laminar premixed hydrogen-added ammonia/air flames for hydrogen production, Int. J. Hydrogen Energy 35 (2010) 1054–1064.
[68] B. Shu, S.K. Vallabhuni, X. He, G. Issayev, K. Moshammer, A. Farooq, R.X. Fernandes, A shock tube and modeling study on the autoignition properties of ammonia at intermediate temperatures, Proc. Combust. Inst. 37 (2019) 205–211.
[69] A.A. Konnov, J. De Ruyck, Kinetic modeling of nitrogen oxides decomposition at flame temperatures, Combust. Sci. Technol. 149 (1999) 53–78.
[70] A.A. Konnov, J. De Ruyck, Kinetic modeling of the thermal decomposition of ammonia, Combust. Sci. Technol. 152 (2000) 23–37.
[71] A.A. Konnov, J. De Ruyck, Kinetic modeling of the decomposition and flames of hydrazine, Combust. Flame 124 (2001) 106–126.
[72] A.A. Konnov, G. Colson, J. De Ruyck, The new route forming NO via NNH, Combust. Flame 121 (2000) 548–550.
[73] A.A. Konnov, J. De Ruyck, Temperature-dependent rate constant for the reaction NNH + O → NH + NO, Combust. Flame 125 (2001) 1258–1264.
[74] A.A. Konnov, G. Colson, J. De Ruyck, NO Formation rates for hydrogen combustion in stirred reactors, Fuel 80 (2001) 49–65.
[75] A.A. Konnov, I.V. Dyakov, J. De Ruyck, Nitric oxide formation in premixed flames of H_2+CO+CO_2 and air, Proc. Combust. Inst. 29 (2002) 2171–2177.
[76] A.A. Konnov, J. De Ruyck, A possible new route for NO formation via N_2H_3, Combust. Sci. Technol. 168 (2001) 1–46.
[77] A.A. Konnov, Implementation of the NCN pathway of prompt-NO formation in the detailed reaction mechanism, Combust. Flame 156 (2009) 2093–2105.
[78] E.N. Volkov, A.A. Konnov, M. Gula, K. Holtappels, A.A. Burluka, Chemistry of NOx decomposition at flame temperatures, Proceedings of the. European Combustion Meeting, Vienna, Austria (2009) CD Paper # 810136, 6 pp, April 14-17.
[79] A.G. Shmakov, O.P. Korobeinichev, I.V. Rybitskaya, A.A. Chernov, D.A. Knyazkov, T.A. Bolshova, A.A. Konnov, Formation and consumption of NO in H_2 + O_2 + N_2 flames doped with NO or NH_3 at atmospheric pressure, Combust. Flame 157 (2010) 556–565.
[80] T. Mendiara, P. Glarborg, Ammonia chemistry in oxy-fuel combustion of methane, Combust. Flame 156 (2009) 1937–1949.
[81] C. Brackmann, V.A. Alekseev, B. Zhou, E. Nordström, P.-.E. Bengtsson, Z. Li, M. Aldén, A.A. Konnov, Structure of premixed ammonia + air flames at atmospheric pressure: laser diagnostics and kinetic modelling, Combust. Flame 163 (2016) 370–381.
[82] M. Abian, M.U. Alzueta, P. Glarborg, Formation of NO from N_2/O_2 mixtures in a flow reactor: toward an accurate prediction of thermal NO, Int. J. Chem. Kinet. 47 (2015) 518–532.
[83] A.A. Konnov, Yet another kinetic mechanism for hydrogen combustion, Combust. Flame 203 (2019) 14–22.
[84] M. Lubrano Lavadera, C. Brackmann, A.A. Konnov, Experimental and modeling study of laminar burning velocities and nitric oxide formation in premixed ethylene/air flames, Proc. Combust. Inst. 38 (2021) 395–404, doi:10.1016/j.proci.2020.06.062.
[85] A. Burcat, B. Ruscic, Third millennium ideal gas and condensed phase thermochemical database for combustion (with updates from active thermochemical tables), Argonne National Laboratory, Argonne, IL, USA, 2005 Report No. ANL-05/20.
[86] D.L. Baulch, C.T. Bowman, C.J. Cobos, R.A. Cox, Th. Just, J.A. Kerr, M.J. Pilling, D. Stocker, J. Troe, W. Tsang, R.W. Walker, J. Warnatz, Evaluated kinetic data for combustion modeling: supplement II, J. Phys. Chem. Ref. Data 34 (2005) 757–1397.
[87] L. Yao, D. Gao, H. Yu, W. Xia, Calculation of the anharmonic effect on the main reactions referring to nitrous oxide in nitrogen-containing combustion mechanism, Chem. Phys. Lett. 751 (2020) 137534.
[88] T.V. Pham, T.J. Tsay, M.C. Lin, Thermal decomposition of N_2O near 900K studied by FTIR spectrometry: comparison of experimental and theoretical O (^{3}P) formation kinetics, Int. J. Chem. Kinet. 52 (2020) 632–644.
[89] W.D. Breshears, Falloff behavior in the thermal dissociation rate of N_2O, J. Phys. Chem. 99 (1995) 12529–12535.
[90] M. Rohrig, E.L. Petersen, D.F. Davidson, R.K. Hanson, The pressure dependence of the thermal decomposition of N_2O, Int. J. Chem. Kinet. 28 (1996) 599–608.
[91] N.E. Meagher, W.R. Anderson, Kinetics of the O(^{3}P) + N_2O reaction. 2. Interpretation and recommended rate coefficients, J. Phys. Chem. A 104 (2000) 6013–6031.
[92] C. Morley, The mechanism of NO formation from nitrogen compounds in hydrogen flames studied by laser fluorescence, Symp. (Int.) Combust. 18 (1981) 23–32.
[93] D.F. Davidson, R.K. Hanson, High temperature reaction rate coefficients derived from N-atoms ARAS measurements and excimer photolysis of NO, Int. J. Chem. Kinet. 22 (1990) 843–861.
[94] L. Adam, W. Hack, H. Zhu, Z.-.W. Qu, R. Schinke, Experimental and theoretical investigation of the reaction NH ($X^3\Sigma^-$) + H (^{2}S) → N (^{4}S) + H_2 ($X^1\Sigma_g^+$), J. Chem. Phys. 122 (2005) 114301.

[95] M. Röhrig, H.G. Wagner, The reactions of NH($X^3\Sigma^-$) with the water gas components CO_2, H_2O, and H_2, Symp. (Int.) Combust. 25 (1994) 975–981.

[96] A. Fontijn, S.M. Shamsuddin, D. Crammond, P. Marshall, W.R. Anderson, Kinetics of the NH reaction with H_2 and reassessment of HNO formation from NH + CO_2, H_2O, Combust. Flame 145 (2006) 543–551.

[97] J.C. Mackie, G.B. Bacskay, Quantum chemical study of the mechanism of reaction between NH ($X\ ^3\Sigma^-$) and H_2, H_2O, and CO_2 under combustion conditions, J. Phys. Chem. A 109 (2005) 11967–11974.

[98] V. Samu, T. Varga, I. Rahinov, S. Cheskis, T. Turányi, Determination of rate parameters based on NH_2 concentration profiles measured in ammonia-doped methane–air flames, Fuel 212 (2018) 679–683.

[99] I. Rahinov, A. Goldman, S. Cheskis, Absorption spectroscopy diagnostics of amidogen in ammonia-doped methane/air flames, Combust. Flame 145 (2006) 105–116.

[100] Y. Li, S.M. Sarathy, Probing hydrogen–nitrogen chemistry: a theoretical study of important reactions in N_xH_y, HCN and HNCO oxidation, Int. J. Hydrogen Energy 45 (2020) 23624–23637.

[101] P. Dransfeld, W. Hack, H. Kurzke, F. Temps, H.Gg Wagner, Direct studies of elementary reactions of NH_2-radicals in the gas phase, Symp. (Int.) Combust. 20 (1985) 655–663.

[102] M-K. Bahng, R.G. Macdonald, Determination of the rate constants for the radical−radical reactions $NH_2(X^{\sim 2}B_1)$ + NH($X^3\Sigma^-$) and $NH_2(X^{\sim 2}B_1)$ + H(^{2}S) at 293K J. Phys. Chem. A 113 (2009) 2415-2423.

[103] D.F. Davidson, K. Kohse-Höinghaus, A.Y. Chang, R.K. Hanson, A pyrolysis mechanism for ammonia, Int. J. Chem. Kinet. 22 (1990) 513–535.

[104] S.J. Klippenstein, L.B. Harding, B. Ruscic, R. Sivaramakrishnan, N.K. Srinivasan, M.-.C. Su, J.V. Michael, Thermal decomposition of NH_2OH and subsequent reactions: ab initio transition state theory and reflected shock tube experiments, J. Phys. Chem. A 113 (2009) 10241–10259.

[105] T. Ko, P. Marshall, A. Fontijn, Rate coefficients for the H + NH_3 reaction over a wide temperature range, J. Phys. Chem. 94 (1990) 1401–1404.

[106] J.V. Michael, J.W. Sutherland, R.B. Klemm, Rate constant for the reaction H + NH_3 over the temperature range 750-1777K, J. Phys. Chem. 90 (1986) 497–500.

[107] G. Altinay, R.G. Macdonald, Determination of the rate constants for the $NH_2(X^2B_1)$ + $NH_2(X^2B_1)$ and $NH_2(X^2B_1)$ + H recombination reactions in n_2 as a function of temperature and pressure, J. Phys. Chem. A 119 (2015) 7593–7610.

[108] G. Altinay, R.G. Macdonald, Determination of the rate constants for the $NH_2(X^2B_1)$ + $NH_2(X^2B_1)$ and $NH_2(X^2B_1)$ + H recombination reactions with collision partners CH_4, C_2H_6, CO_2, CF_4, and SF_6 at low pressures and 296K. Part 2, J. Phys. Chem. A 116 (2012) 2161–2176.

[109] A.W. Jasper, J.A. Miller, S.J. Klippenstein, Collision efficiency of water in the unimolecular reaction CH_4 (+H_2O) CH_3 + H (+H_2O): one-dimensional and two-dimensional solutions of the low-pressure-limit master equation, J. Phys. Chem. A117 (2013) 12243–12255.

[110] D.P. Linder, X. Duan, M. Page, Thermal rate constants for R+N_2H_2→RH+N_2H (R=H, OH, NH_2) determined from multireference configuration interaction and variational transition state theory calculations, J. Chem. Phys. 104 (1996) 6298–6307.

[111] J. Zheng, R.J. Rocha, M. Pelegrini, L.F.A. Ferrão, E.F.V. Carvalho, O. Roberto-Neto, F.B.C. Machado, D.G. Truhlar, A product branching ratio controlled by vibrational adiabaticity and variational effects: kinetics of the H + trans-N_2H_2 reactions, J. Chem. Phys. 136 (2012) 184310.

[112] M. Döntgen, K. Leonhard, Discussion of the separation of chemical and relaxational kinetics of chemically activated intermediates in master equation simulations, J. Phys. Chem. A121 (2017) 1563–1570.

[113] A.M. Dean, J.W. Bozzelli, Combustion chemistry of nitrogen, in: W.C. Gardiner (Ed.), Gas-phase Combustion Chemistry, Springer, New York (2000), pp. 125–341.

[114] P. Marshall, A. Fontijn, C.F. Melius, High-temperature photochemistry and BAC-MP4 studies of the reaction between ground-state H atoms and N_2O, J. Chem. Phys. 86 (1987) 5540–5549.

[115] J.W. Bozzelli, A.Y. Chang, A.M. Dean, Analysis of the reactions H+N_2O and NH+NO: pathways and rate constants over a wide range of temperature and pressure, Symp. (Int.) Combust. 25 (1994) 965–974.

[116] E.W.G. Diau, M.C. Lin, Theoretical study of H(D) + N_2O: effects of pressure, temperature, and quantum-mechanical tunneling on H(D)-atom decay and OH(D)-radical production, J. Phys. Chem. 99 (1995) 6589–6594.

[117] S.J. Klippenstein, L.B. Harding, P. Glarborg, J.A. Miller, The role of NNH in NO formation and control, Combust. Flame 158 (2011) 774–789.

[118] Y. Hidaka, H. Takuma, M. Suga, Shock-tube study of the rate constant for excited OH* ($^2\Sigma^+$) formation in the N_2O-H_2 reaction, J. Phys. Chem. 89 (1985) 4903–4905.

[119] T. Rutar, J.C. Kramlich, P.C. Malte, P. Glarborg, Nitrous oxide emissions control by reburning, Combust. Flame 107 (1996) 453–463.

[120] E.W. Diau, M.J. Halbgewachs, A.R. Smith, M.C. Lin, Thermal reduction of NO by H_2: kinetic measurement and computer modeling of the HNO + NO reaction, Int. J. Chem. Kinet. 27 (1995) 867–881.

[121] A.M. Mebel, M.C. Lin, K. Morokuma, C.F. Melius, Theoretical study of reactions of N_2O with NO and OH radicals, Int. J. Chem. Kinet. 28 (1996) 693–703.

[122] R.K. Hanson, S. Salimian, Survey of rate constants in the N/H/O system, in: W.C. Gardiner (Ed.), Combustion Chemistry, Springer, New York (1984), p. 361.

[123] N. Cohen, K.R. Westberg, Chemical kinetic data sheets for high-temperature reactions. Part II, J. Phys. Chem. Ref. Data 20 (1991) 1211–1311.

[124] R. Sumathi, D. Sengupta, M.T. Nguyen, Theoretical study of the H_2 + NO and related reactions of [H_2NO] isomers, J. Phys. Chem. A 102 (1998) 3175–3183.

[125] S. Inomata, N. Washida, Rate constants for the reactions of NH_2 and HNO with atomic oxygen at temperatures between 242 and 473K, J. Phys. Chem. A 103 (1999) 5023–5031.

[126] G. Hennig, M. Klatt, B. Spindler, H.G.G. Wagner, The reaction of NH_2+O_2 at high temperatures, Berichte der Bunsengesellschaft für physikalische Chemie 99 (1995) 651–657.

[127] J.A. Miller, P. Glarborg, Modeling the thermal De-NO_x process: closing in on a final solution, Int. J. Chem. Kinet. 31 (1999) 757–765.

[128] S. Song, R.K. Hanson, C.T. Bowman, D.M. Golden, Shock tube determination of the overall rate of NH_2 + NO → products in the thermal De-NOx temperature window, Int. J. Chem. Kinet. 33 (2001) 715–721.

[129] T.L. Nguyen, J.F. Stanton, High-level theoretical study of the reaction between hydroxyl and ammonia: accurate rate constants from 200 to 2500K, J. Chem. Phys. 147 (2017) 152704.

[130] W. Tsang, J.T. Herron, Chemical kinetic data base for propellant combustion. I. Reactions involving NO, NO_2, HNO, HNO_2, HCN and N_2O, J. Phys. Chem. Ref. Data 20 (1991) 609–663.

[131] M.T. Allen, R.A. Yetter, F.L. Dryer, Hydrogen/nitrous oxide kinetics-Implications of the N_xH_y species, Combust. Flame 112 (1998) 302–311.

[132] P. Glarborg, M. Østberg, M.U. Alzueta, K. Dam-Johansen, J.A. Miller, The recombination of hydrogen atoms with nitric oxide at high temperatures, Symp. (Int.) Combust. 27 (1998) 219–226.

[133] P.S. Riley, B. Cosic, A. Fontijn, The H+NO recombination reaction over a wide temperature range, Int. J. Chem. Kinet. 35 (2003) 374–380.

[134] C.L. Rasmussen, J. Hansen, P. Marshall, P. Glarborg, Experimental measurements and kinetic modeling of CO/H_2/O_2/NO_x conversion at high pressure, Int. J. Chem. Kinet. 40 (2008) 454–480.

[135] M.R. Soto, M. Page, M.L. McKee, Theoretical study of the reaction of OH with HNO, Chem. Phys. 153 (1991) 415–426.

[136] M.R. Soto, M. Page, Ab initio variational transition-state-theory reaction-rate calculations for the gas-phase reaction H+HNO→H_2+NO, J. Chem. Phys. 97 (1992) 7287–7296.

[137] H.M.T. Nguyen, S. Zhang, J. Peeters, T.N. Truong, M.T. Nguyen, Direct ab initio dynamics studies of the reactions of HNO with H and OH radicals, Chem. Phys. Lett. 388 (2004) 94–99.

[138] S. Xu, M.C. Lin, Ab initio chemical kinetics for the NH_2 + HNO_x reactions, part I: kinetics and mechanism for NH_2 + HNO, Int. J. Chem. Kinet. 41 (2009) 667–677.

[139] A.M. Mebel, E.W.G. Diau, M.C. Lin, K. Morokuma, Theoretical rate constants for the NH_3 + NO_x → NH_2 + HNO_x (x = 1, 2) reactions by ab initio MO/VTST calculations, J. Phys. Chem. 100 (1996) 7517–7525.

[140] J.W. Bozzelli, A.M. Dean, N.N.H. O +, A Possible new route for NO_x formation in flames, Int. J. Chem. Kinet. 27 (1995) 1097–1109.

[141] N.L. Haworth, J.C. Mackie, G.B. Bacskay, An ab initio quantum chemical and kinetic study of the NNH + O reaction potential energy surface: how important is this route to NO in combustion? J. Phys. Chem. A 107 (2003) 6792–6803.

[142] P. Glarborg, J.E. Johnsson, K. Dam-Johansen, Kinetics of homogeneous nitrous oxide decomposition, Combust. Flame 99 (1994) 523–532.

[143] O.E. Krivonosova, S.A. Losev, V.P. Nalivaiko, Yu.K. Mukoseev, O.P. Shatalov, Recommended data on the rate constants of the chemical reactions between molecules consisting of N and O atoms, Plasma Chemistry, 14, Energoatomizdat, Moscow (1987), pp. 3–31. (In Russian).

[144] A. Ichikawa, A. Hayakawa, Y. Kitagawa, K.D. Kunkuma Amila Somarathne, T. Kudo, H. Kobayashi, Laminar burning velocity and Markstein length of ammonia/hydrogen/air premixed flames at elevated pressures, Int. J. Hydrogen Energy 40 (2015) 9570–9578.

[145] C. Lhuillier, P. Brequigny, N. Lamoureux, F. Contino, C. Mounaïm-Rousselle, Experimental investigation on laminar burning velocities of ammonia/hydrogen/air mixtures at elevated temperatures, Fuel 263 (2020) 116653.